INFORMATION TO USERS

This manuscript has been reproduced from the microfilm master. UMI films the text directly from the original or copy submitted. Thus, some thesis and dissertation copies are in typewriter face, while others may be from any type of computer printer.

The quality of this reproduction is dependent upon the quality of the copy submitted. Broken or indistinct print, colored or poor quality illustrations and photographs, print bleedthrough, substandard margins, and improper alignment can adversely affect reproduction.

In the unlikely event that the author did not send UMI a complete manuscript and there are missing pages, these will be noted. Also, if unauthorized copyright material had to be removed, a note will indicate the deletion.

Oversize materials (e.g., maps, drawings, charts) are reproduced by sectioning the original, beginning at the upper left-hand corner and continuing from left to right in equal sections with small overlaps.

ProQuest Information and Learning
300 North Zeeb Road, Ann Arbor, MI 48106-1346 USA
800-521-0600

PHASE EQUILIBRIA OF SIMPLE FLUIDS AT CRYOGENIC TEMPERATURES

BY

DENIS V. GRAVELLE

A THESIS SUBMITTED IN PARTIAL FULLFILLMENT

OF THE REQUIREMENT FOR THE DEGREE OF

MASTER OF APPLIED SCIENCE

IN THE

DEPARTMENT OF CHEMICAL ENGINEERING

UNIVERSITY OF OTTAWA

OTTAWA, CANADA

OCTOBER, 1969

RESEARCH DIRECTOR

M.A.Sc. CANDIDATE

ABSTRACT

Isothermal vapour-liquid equilibrium measurements have been measured by a forced-recirculation type of apparatus; the temperature range investagated being 115-137 °K for the binary system argon-methane and at 123.44 °K for the ternary system argon-nitrogen-methane.

Results were presented in the form of activity coefficients γ as a function of compositions; high pressure and low pressure equations being used in their determinations.

Binary and ternary constants for the one-suffix Redlich-Kister equation have been found to represent both the binary and ternary data adequately.

Experimental data were examined for consistency by noting the trend of the terminal values of the activity coefficients at the investigated temperatures.

Owing to scarce literature data pertaining to the ternary effect, a qualitative treatment has been made.

ACKNOWLEDGEMENT

The author is gratefully indedted to Dr. B.C.-Y. Lu for directing this research work and providing valuable suggestions as to the conduct of the experiment. His morale encouragement and continued interest in the performance of this study have been deeply appreciated.

He also wishes to express his appreciation to S.-D. Chang for sharing his experience on computer applications and providing helpful advice as to the various methods of analysis.

The aid of G. Gasperetti and F. Giacobbi in certain phases of the setting up of the experimental equipment is gratefully acknowledged. Also many thanks are extended to G. Brunet for his fine clerkship and to M. Gravelle for his benevolence in typing most of this thesis.

The author also wishes to thank the National Research Council of Canada for financial support.

LIST OF FIGURES

LIST OF TABLES

NOMENCLATURE

AA	Cheung and Wang temperature correlation coefficient
a, b	Parameters of the Redlich-Kwong equation of state
B	One-suffix Redlich-Kister constant
C	Two-suffix Redlich-Kister constant
C_{123}	Ternary constant
f	Fugacity
G	Gibb's free energy
K	Equilibrium constants y/x, and degree Kelvin
k	Interaction coefficient of the critical temperature characteristic
N	Number of experimental points
P	Pressure
Q	'Q function' describing excess free energy
R	Universal gas constant
T	Temperature
V	Total volume of gas mixture
v	Molar volume
x	Liquid mole fraction
g	Vapour mole fraction
Z	Compressibility factor characteristic
$\% D_a$	Percent deviation in activity coefficient for component a

GREEK LETTERS

β, $\beta\beta$	second and third virial coefficients
γ	activity coefficient
Ω	dimensionless parameters of the Redlich-Kwong equation of state
σ	standard deviation
μ	chemical potential

NOMENCLATURE (continued)

ϕ	fugacity coefficient
ω	accentric factor
Ψ	reference fugacity at the critical pressure
Δ	difference or property change on mixing

SUBSCRIPTS

a, b	pertaining to the Redlich-Kwong equation of state dimensionless parameters
c	critical properties
i, j, k,	component identification
ii, jj, ij	component interaction or critical property characteristic
L	liquid phase
V	vapour phase
r	reduced properties
1	argon
2	nitrogen
3	methane
1, 2	equation coefficient identification

SUPERCRIPTS

-	partial molar property
^	solution property
—	average value
•	reference state, zero pressure and degree
calc	calculated value
E	excess property
obs	observed value
Po	zero pressure

NOMENCLATURE (continued)

P_s	saturation pressure
P_r	reference pressure
s	saturation condition

TABLE OF CONTENTS

TABLE OF CONTENTS (continued)

TABLE OF CONTENTS (continued)

I. INTRODUCTION

The ever-increasing technological progress of the chemical industries have oriented researchers to subject vapour-liquid equilibrium data at high pressures to thermodynamic analysis. The ultimate goal of this orientation is to close the gap existing between the empiricity of industrial applications and the theoretical predictions of such processes.

Accuracy in the prediction of thermodynamic properties has been limited to that of a suitable equation of state which can describe liquid and vapour behaviour.

A suitable equation of state can be used to estimate thermodynamic functions such as activity coefficients. This function can be related to easily measurable intensive properties of temperature, pressure and composition.

The objective of this work has been limited to the observation of such properties; that is, the pressure-composition behaviour with temperature were studied. With the existing knowledge on phase behaviour, it was possible to correlate the activity coefficients with temperature for the binary system argon-methane. Extension to the ternary system of argon-nitrogen-methane was then possible. The possibility of interaction among the constituents was analysed from the behaviour of the binary pairs constituting the ternary system.

II. LITERATURE SURVEY

In view of the fact that bibliographies [30,31] available are quite exhaustive and up to date, only a brief review of the literature will be made in this thesis, covering only those systems which are of interest to this study.

Related works on vapour-liquid equilibrium is briefly reviewed for $Ar-CH_4$ and $Ar-CH_4-N_2$ mixtures at cryogenic temperature.

Scarce data (7 points) on $Ar-CH_4$ system was obtained in 1964 by Cheung and Wang [1] at temperatures of 114.5°K and 123.9°K. However, the range covered on a P-x-y diagram is only up to 22% argon.

In 1966, equilibrium data for the binary and ternary system were obtained by Sprow and Prausnitz [2,3]. The temperature investigated was 90.67°K. At this point, work done by Pool et al. [4] in 1962 should be mentioned. Several systems were investigated, one of them being $Ar-N_2$ at 82.82°K. Actually, the data obtained for that particular system was compared against those obtained with the apparatus developed by the Sprow group.

A binary system of $Ar-CH_4$ was also studied by K.K. Maitra, a former graduate student of this department [5]. The isotherms studied were 123, 133 and 143°K. This work could not have been made possible without the splendid effort of S.-D. Chang in 1963 [6].

He introduced for the first time in our laboratory the forced-recirculation apparatus with his personal contribution to improve it over others used in different research establishments. His contribution proved to be highly successful. In 1967, a scientific paper by Chang and and Lu [7] was published. It illustrated the experimental equipment and exhibited the P-x-y data for mixtures of $N_2-CH_4-C_2H_6$. In the present work,

a very similar apparatus was used to study the systems already mentioned. The principle and arrangement of the forced-recirculation apparatus is the same except for a few sophisticated equipment added to improve somewhat, its performance.

It may also be mentioned that recently, the Van't Zelfde group [8] investigated the vapour-solid-liquid equilibrium of Ar-CH_4 system between temperatures of 71-90.6°K.

III. THEORETICAL CONSIDERATIONS

III.1 INTRODUCTION

A criterion of equilibrium requires that at constant temperature and pressure the chemical potential of component i in the vapour phase, $\mu_{i,V}$, be equal to that in the liquid phase, $\mu_{i,L}$:

$$\mu_{i,V} = \mu_{i,L}$$

It follows that the fundamental equation of vapour-liquid equilibrium is conveniently written in terms of fugacities; for each component i, the fugacity in the vapour phase, $\hat{f}_{i,V}$ is equal to that in the liquid phase, $\hat{f}_{i,L}$:

$$\hat{f}_{i,V} = \hat{f}_{i,L} \qquad (1)$$

III.2 LOW-PRESSURE PHASE EQUILIBRIA

At low pressures - up to several atmospheres - certain quite reliable assumptions can be made about the behaviour of the vapour phase. This allows the development of an adequate equation for the calculation of liquid-phase activity coefficients from phase-equilibrium data. Equation (1) and the definition of activity coefficient for either the liquid or vapour phase can be used to develop an expression for the activity coefficients [9]. For component i,

$$\ln\gamma_{i,L} = \ln\frac{y_i P}{x_i P_i^s} + \frac{(\beta_{ii} - v_{i,L})(P - P_i^s)}{RT} + \frac{P y_i (2\beta_{ij} - \beta_{ii} - \beta_{jj})}{RT} \qquad (2)$$

where β_{ii} and β_{ij} are respectively, the second virial coefficient of the pure constituent and the second cross-virial coefficient of the i-j interaction. The liquid molar volume and the vapour pressure of the component at temperature T, are respectively, $v_{i,L}$ and P_i^s .

The second virial and cross-virial coefficients may either be obtained from literature [10] or from correlation [11].

III.3 HIGH-PRESSURE PHASE EQUILIBRIA

High-pressure phase equilibria deals with a more complex problem. Thus, to facilitate thermodynamic analysis, two auxiliary functions [9] are introduced; the vapour-phase fugacity coefficient ϕ_i and the liquid phase activity coefficient γ_i :

$$\hat{f}_{i,V} = \phi_i y_i P \tag{3}$$

$$\hat{f}_{i,L} = \gamma_i x_i f_i^{\circ} \tag{4}$$

where y and x are respectively, mole fractions in the vapour phase and in the liquid phase, P is the total pressure and f_i° is the standard-state fugacity of pure component i.

At equilibrium, $\hat{f}_{i,L} = \hat{f}_{i,V}$; then Equation (3) and Equation (4) may be combined to give:

$$\gamma_i = \frac{\phi_i y_i P}{x_i f_i^{\circ}} \tag{5}$$

III.4 VAPOUR-PHASE MOLAR VOLUME

The vapour-phase fugacity coefficients may be obtained from an equation of state. One of minimum complexity is the Redlich-Kwong equation of state [32] :

$$P = \frac{RT}{v - b} - \frac{a}{T^{0.5} v(v + b)} \tag{6}$$

where

$$a = \frac{\Omega_a R^2 T_c^{2.5}}{P_c} \qquad \text{and}$$

$$b = \frac{\Omega_b R T_c}{P_c} \quad .$$

The parameters 'a' and 'b' are determined by imposing the existence of critical conditions on Equation (6). The dimensionless constants are $\Omega_a = 0.4278$ and $\Omega_b = 0.0867$.

The constants of the Redlich-Kwong equation of state for temperatures below the critical point are represented by the following set of equations: (12,13)

$$b = \sum_i^n y_i b_i$$

and

$$a = \sum_i^n \sum_j^n y_i y_j a_{ij}$$

where

$$b_i = \frac{\Omega_{b,i} R T_{c,i}}{P_{c,i}} \quad ,$$

and

$$a_{ii} = \Omega_{a,i} R^2 T_{c,i}^{2.5} \quad ,$$

$$a_{ij} = \frac{(\Omega_{a,i} + \Omega_{a,j}) R^2 T_{c,ij}^{2.5}}{2 P_{c,ij}}$$

The critical pressure, temperature and volume characteristics are given by

$$P_{c,ij} = \frac{Z_{c,ij} R T_{c,ij}}{V_{c,ij}} \quad ,$$

$$T_{c,ij} = \sqrt{T_{c,ii} T_{c,jj}} \; (1 - k_{ij}) \qquad \text{and}$$

$$v_{c,ij} = \left(\frac{1}{2} \left(v_{c,i}^{1/3} + v_{c,j}^{1/3} \right) \right)^3 \quad .$$

Along the same line, the compressibility factor characteristic is related to the accentric factor ω_i and ω_j :

$$Z_{c,ij} = 0.291 - 0.08 \left(\frac{\omega_i + \omega_j}{2} \right) \quad .$$

The molar volume, v, is that of the gas mixture and is obtained by solving Equation (6) (which is cubic in v) and taking the largest real root for v. The dimensionless constants $\Omega_{a,i}$ and $\Omega_{b,i}$ are those for saturated vapour of each component.

III.5 VAPOUR-PHASE FUGACITY COEFFICIENT

As indicated by Equation (3), the fugacity of a component i in a gas mixture is related to the total pressure P and its vapour mole fraction y_i through the fugacity coefficient ϕ_i. The fugacity coefficient is a function of pressure, temperature and gas composition; it is related to the volumetric properties of the gas mixture by the exact relation [15]

$$\ln \phi_i = \frac{1}{RT} \int_o^\infty \left[\left(\frac{\partial P}{\partial n_i} \right)_{T,P,n_j} - \frac{RT}{V} \right] dV - \ln Z \qquad (7)$$

where V is the total volume of the gas mixture. By substituting the modified Redlich-Kwong equation of state (Equation (6)) into Equation (7), the fugacity coefficient of component k in the mixture becomes [16] :

$$\ln \phi_k = \ln \frac{v}{v-b_k} + \frac{b_k}{v-b_k} - 2 \frac{\sum y_i a_{ik}}{RT^{3/2} b_k} \ln \left(\frac{v+b_k}{v} \right) + \frac{ab_k}{RT^{3/2} b_k^2} \left(\ln \frac{v+b_k}{v} - \frac{b_k}{v+b_k} \right) - \ln Z \qquad (8)$$

It has been reported [16] that Equation (8) is useful for T_r less than 0.91.

III.6 LIQUID-PHASE REFERENCE FUGACITY

An activity coefficient is meaningless unless accompanied with a detailed description of the standard state to which it refers. Various methods or correlations for obtaining the standard fugacity have been reported by many observers (17, 18).

The choice of the standard state of a constituent is arbitrary within the restrictions that it must always be at the solution temperature and that it must be at a state of fixed pressure and composition.

For subcritical conditions, the most commonly used reference state composition is describe by

$$\lim_{x_i=1} \gamma_i = 1 \qquad (9)$$

It is known as the symmetrical convention.

The reference pressure is always selected on an arbitrary basis, say, saturation pressure P^s.

The reference fugacity may be corrected to zero pressure by

$$\left(\frac{\partial \ln f_i}{\partial P}\right)_{T,x} = \frac{v_{i,L}}{RT} \qquad (10)$$

where v_i is the molar volume of component i. In other words; at the experimental temperature T, and the composition expressed by Equation (9), it is possible to correct the reference fugacity to zero pressure by integration of Equation (10) between the limits ($P = P^\circ$, $P = P^s$) where P^s is the saturation pressure at temperature T and P° is zero pressure. Then,

$$f_i^{Po} = f_i^{Ps} \, EXP\left(-\frac{v_{i,L} P^s}{RT}\right)$$

With $y_i = 1$ and Equation (3),

$$f_i^{Ps} = \phi_{pure\ i}\, P^s \quad .$$

Therefore,

$$f_i^{Po} = \frac{\phi_{pure\ i}\, P^s}{EXP\ \frac{v_{i,L}\, P^s}{RT}} \quad , \tag{11}$$

where f_i^{Po} is the reference fugacity evaluated at zero pressure when the reference pressure is at saturation. Equation (11) holds for reduced temperature less than 0.91. [12,13,16]

Along the same line, Lyckman's et.al, [18] defines a quantity

$$\psi = \frac{f_i^{Po}}{P_{c,i}} \tag{12}$$

for reduced pressure greater than 0.56, the reference state being zero pressure. A generalized reference fugacity for the liquid phase was based on a three-parameter theory of corresponding states and was expressed in a form suggested by Pitzer et,al, [20] :

$$\log\psi = (\log\psi)_1 + \omega(\log\psi)_2 \tag{13}$$

where $(\log\psi)_1$ and $(\log\psi)_2$ are each functions of the reduced temperature.

III.7 LIQUID-PHASE ACTIVITY COEFFICIENT

When the standard state fugacity is defined at a constant pressure, then for any component i, the pressure dependence of the activity coefficient is given by :

$$\left(\frac{\partial \ln\gamma_i}{\partial P}\right)_{T,x} = \frac{\bar{v}_i}{RT} \tag{14}$$

where $\bar{v}_i$ is the partial molar volume of component i. Integrating Equation (14) between limits of the arbitrary reference pressure Pr and the experimental pressure P, we have:

$$\gamma_i^{Pr} = \gamma_i^{P} \, EXP\left[- \int_{Pr}^{P} \left(\frac{\bar{v}_i}{RT} \right) dp \right] \tag{15}$$

where γ_i^{Pr} is the activity coefficient of component i at temperature T and composition x_i, corrected to any arbitrary pressure Pr . To be consistent with Equation (11), Pr = Po, and Equation (15) becomes

$$\gamma_i^{Po} = \gamma_i^{P} \, EXP\left[- \int_{o}^{P} \left(\frac{\bar{v}_i}{RT} \right) dp \right] \tag{16}$$

With the assumption of pressure independent partial molar volume, Equation (16) becomes

$$\gamma_i^{Po} = \gamma_i^{P} \, EXP \left(- \frac{\bar{v}_i P}{RT} \right) \tag{17}$$

The activity coefficient γ_i^{P} is given by Equation (5), except that $f_i^{*} = f_i^{Po}$. Therefore,

$$\gamma_i^{Po} = \frac{\phi_i y_i P}{x_i f_i^{Po}} \tag{5}$$

It follows that for a specific case, the corrected activity coefficient to P = 0 is represented by

$$\gamma_i^{Po} = \frac{\phi_i y_i P}{x_i f_i^{Po} EXP\left(\frac{\bar{v}_i P}{RT} \right)} \tag{18}$$

or, more generally, by Equation (15). Equation (18) may be solved by

making use of Equation (8) for ϕ_i, Equation (12) for f_i^{Po} if Lyckman's correlation is used or Equation (11) where no correlations are needed and, lastly, the experimental P-x-y data.

III.8 MODERATE PRESSURE VAPOUR-LIQUID EQUILIBRIA

Low pressure activity coefficients may be represented by Equation (2), however, many assumptions are made before the final form is arrived at.

The substitution of the virial equation,

$$\frac{Pv}{RT} = 1 + \frac{\beta}{v} + \frac{\beta\beta}{v^2} + \frac{\beta\beta\beta}{v^3} + \cdots\cdots ,$$

into the exact relation for fugacity coefficient as given by Equation (7), may prove to be more representative of the activity coefficients obtained through Equation (18).

Much information is available on the second virial coefficients for the argon-methane system [10,11], and a limited amount [33,34] is known about the third virial coefficient; almost nothing is known about the fourth or higher virial coefficients [33]. For all practical purposes therefore, the series in v of the virial equation can be cut off after the third term.

In a mixture the second and third virial coefficients, β and $\beta\beta$ respectively, are function of temperature and composition and are given by

$$\beta_{mix} = \sum_i^n \sum_j^n y_i y_j \beta_{ij}$$

$$\beta\beta_{mix} = \sum_i^n \sum_j^n \sum_k^n y_i y_j y_k \beta\beta_{ijk} .$$

Substitution of the virial equation with corresponding expressions of the virial coefficients into Equation (7) yield the following exact relation

$$\ln\phi_i = \frac{2}{v}\sum_j^n y_j\beta_{ij} + \frac{3}{2v^2}\sum_j^n\sum_k^n y_i y_k \beta\beta_{ijk} - \ln Z \qquad (19)$$

This equation is exact as long as v is sufficiently large to permit neglect of terms involving the fourth and higher virial coefficients. It is also limited to a certain pressure range because of the presence of the virial coefficients. Correlations of the third virial coefficients are scarce [33], however, can be compared against those experimentally obtained[34,27].

III.9 CONSISTENCY TEST

A rigorous and general consistency test was proposed by Chang and Lu[6], [23] to examine experimental data. The equations do not involve activity coefficient terms and are applicable to all conditions including the situation when the system temperature is above the critical temperature of the more volatile component. They reported that the proposed method is sensitive to errors in the composition measurements and insensitive to the supporting data employed in the point-by-point evaluation of the experimental data.

The overall deviation resulting from experimental errors of the tested pair was reported as

$$\Delta = \sum_i^n (x_{i,b} + x_{i,a})\left[\ln\left(\frac{K_{i,b}}{K_{i,a}}\right) - \ln\frac{\phi_{i,a}P_a}{\phi_{i,b}P_b} - \int_{P_a}^{P_b}\left(\frac{\bar{v}_{i,L}}{RT}\right)dp\right] \qquad (20a)$$

In order to make a test conclusive, maximum experimental error bounds must be established. As all measured results have experimental errors, it is necessary to determine whether or not the data are consistent within error bounds . For the points to be consistent, the maximum experimental

error bounds must be less than the overall deviation expressed by Equation (20a).

The maximum experimental error bounds for isothermal data was represented by the following equation:

$$D_{max} = \sum_{i}^{n} (x_{i,b} + x_{i,a}) \left[\left(\frac{1}{y_{i,a}} + \frac{1}{y_{i,b}} + \frac{1}{x_{i,a}} + \frac{1}{x_{i,b}} \right) + \right.$$

$$2 \left| \left(\ln \left(\frac{K_{i,b}}{K_{i,a}} \right) - \ln \left(\frac{\phi_{i,a} P_a}{\phi_{i,b} P_b} \right) - \int_{P_a}^{P_b} \left(\frac{\bar{v}_{i,L}}{RT} \right) dp \right| \right) E(x) +$$

$$\sum_{i}^{n} (x_{i,b} + x_{i,a}) \left(\frac{1}{P_a} + \frac{1}{P_b} + \left| \frac{\partial}{\partial P} \int_{P_a}^{P_b} \left(\frac{\bar{v}_{i,L}}{RT} \right) dp \right| \right) E(P) +$$

$$\sum_{i}^{n} (x_{i,b} + x_{i,a}) \left| \left(\frac{\partial}{\partial T} \int_{P_a}^{P_b} \left(\frac{\bar{v}_{i,L}}{RT} \right) dp \right) \right| E(T) \qquad (20b)$$

where E(x) is the error in composition measurement, E(P) is the error in pressure measurement, E(T) is the error in temperature measurement.

III.10 REDLICH-KISTER EQUATION

The Redlich-Kister Equation are the most commonly used equations for relating liquid activity coefficients with liquid compositions.

The authors [25] introduced the quantity

$$Q = \frac{\Delta G^E}{2.303\ RT}$$

For a n-component system the 'Q function' becomes

$$Q_{i..n} = \sum_{i}^{n} x_i \log \gamma_i \qquad (21a)$$

Redlich and Kister proposed that Q be represented by an appropriate power series of the liquid composition, the expansion for a binary system being

$$Q_{ij} = x_i x_j \left[B_{ij} + C_{ij}(x_i - x_j) + D_{ij}(x_i - x_j)^2 + \ldots\ldots \right] \quad (21b)$$

where the constants B_{ij} , C_{ij} , D_{ij} , are temperature dependent only.

By differentiation of Equation (21a) with respect to composition, the individual activity coefficients may be conveniently represented.

III.10-a BINARY SYSTEM

For binary systems, the expressions relating liquid activity coefficients to the liquid compositions are:

$$\log\gamma_i = x_j^2(B_{ij} + C_{ij}(3x_i - x_j) + \ldots\ldots) \quad (22)$$

and

$$\log\gamma_j = x_i^2(B_{ij} + C_{ij}(x_j - 3x_i) + \ldots\ldots) \quad (23)$$

These expressions may be least-square fitted to ' P, x_i, $\log\gamma_i$, $\log\gamma_j$ ' observed data at a given temperature.

The selection of the proper suffix equation depends on the molecular complexity of the system and the precision of the experimental data.

Another basis for selection is the standard deviation in γ_i for individual suffixed equation given by the familiar

$$\sigma_i = \sqrt{\frac{\sum_i^N (\gamma_i^{calc} - \gamma_i^{obs})^2}{N - n}}$$

where N and n are respectively, the number of experimental points and the degree of freedom. γ_i^{calc} and γ_i^{obs} are respectively, the calculated γ_i from the constants B_{ij}, C_{ij}, etc., obtained by least-square fitting of the Equations (22) and (23), and the computed γ_i from either high or low pressure equations.

III.10-b TERNARY SYSTEM

For a ternary system the function Q can be expressed as follows :

$$Q_{123} = x_1 \log \gamma_1 + x_2 \log \gamma_2 + x_3 \log \gamma_3 \qquad (25)$$

which may be obtained from observed data.

The function Q_{123} can also be represented as the sum of Equation (21b) for all three binary systems involved plus terms representing the possible interaction among different molecules.

For example, all three binary systems obeying the one-suffix Redlich-Kister equations, the Q function may be represented by

$$Q_{123} = x_1 x_2 B_{12} + x_2 x_3 B_{23} + x_3 x_1 B_{31} + x_1 x_2 x_3 C_{123} \qquad (26)$$

where C_{123} is the interaction effect. For simple systems C_{123} should be close to zero suggested by Pigford [26]. To determine C_{123} Equations (25) and (26) are used.

Whenever one or more of the binary systems require the use of n-suffix equations, the multicomponent equations should also be of the n-suffix variety, but the ternary effects may be no more complicated in these cases than they are for systems with simpler binary component systems.

Severns [26] reported a positive sign of C_{123}. It entered an equation similar to Equation (26) in such a way as to lower the excess free energy. This lowering in excess free energy may be attributed to the formation of ternary aggregate. Furthermore, they indicated unlikely that significant negative values of C_{123} in Equation (26) would occur in any ternary system.

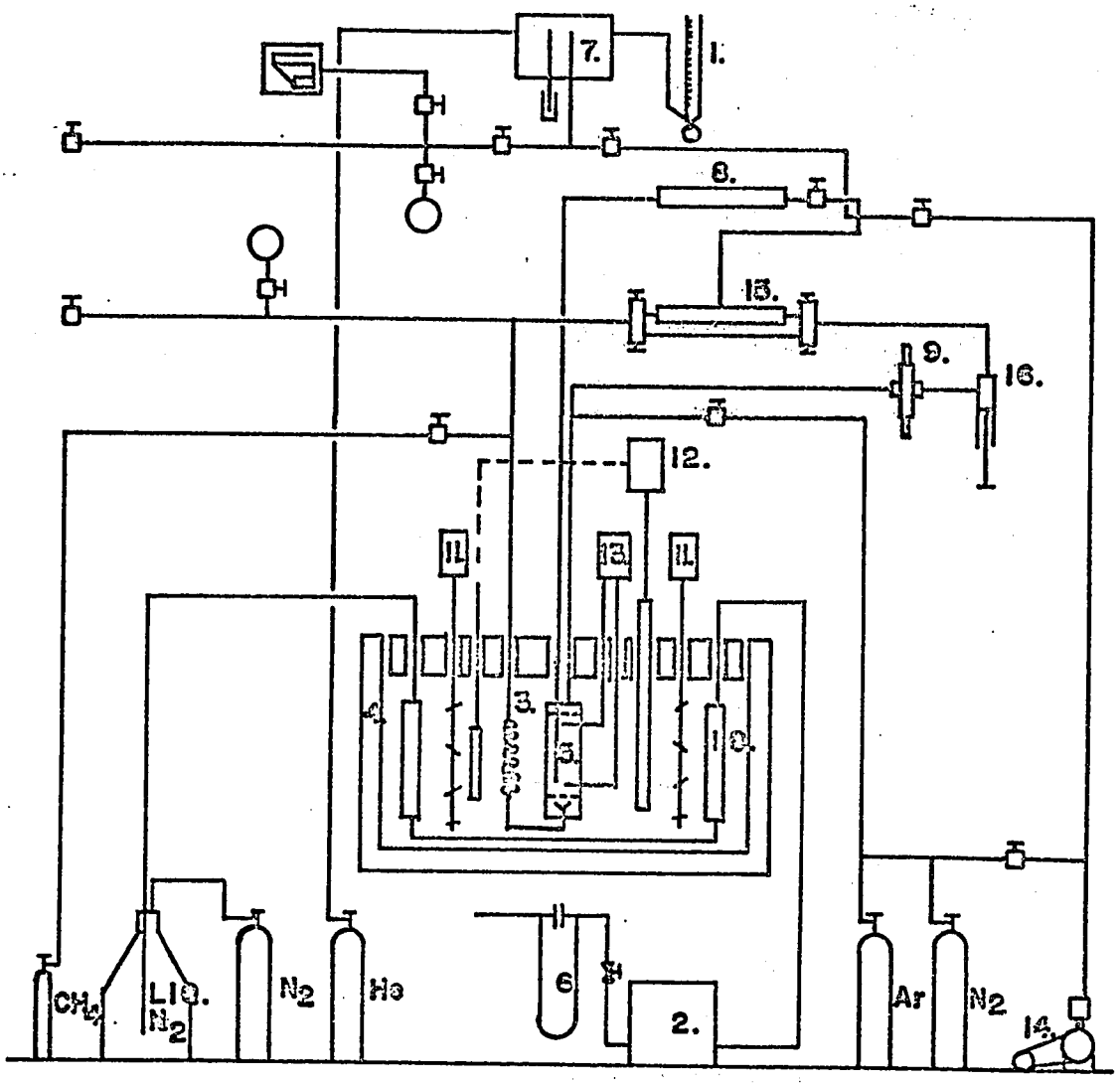

1_BUBBLE TOWER
2_BUFFER TANK
3_CONDENSATION COIL
4_ CRYOSTAT
5_ EQUILIBRIUM CELL
6_FLOW INDICATOR
7_GAS CHROMATOGRAPH
8_LIQ. SAMPLING TUBE
9_ELECTROMAGNETIC PUMP
10_ N_2 VAPORIZATION COIL
11_ELECTRIC STIRRER
12_TEMP. CONTROLER
13_THERMOCOUPLE ASSEMBLY
14_ VACUUM PUMP
15_ VAP. SAMPLING TUBE
16_ VOLUME REGULATOR

FIGURE (1) : THE FORCED-RECIRCULATION APPARATUS

IV. EXPERIMENTAL DETAILS

IV.1 INTRODUCTION

A schematic diagram of the forced-recirculation apparatus used in this study is shown in Figure (1).

To fully appreciate the details involved in the description of the equipment, the discussion will be presented in three sections.

The equilibrium system and the sampling system are first depicted. To interrelate these functional units, aspects and uses of the controlling and measuring devices are not to be avoided. Consequently, an ensemble of the apparatus is at hand to give it a just conception when it is used in the study of vapour-liquid equilibria [6].

IV.2 EQUILIBRIUM SYSTEM

The recirculation loop of the equilibrium system is a high vacuum space into which the gaseous solution to be analysed at equilibrium conditions is introduced. The solution may be any of a pure component, a binary or multicomponent mixture. Part of the loop is submerged into the constant temperature cryostat, the other section being located in ambient temperature. The four main parts of the cylce are described henceforth.

The schematized drawing of the recirculation loop on Figure (2) illustrates the main units of the cycle. The nucleus of the four functional parts of the recirculation loop is the equilibrium cell.

Both the equilibrium cell and the condensing coil are immersed in an isopentane bath. The 20-liter cryostat is maintained at a constant temperature. The electromagnetic pump and the volume regulator are located outside the cryostat at room temperature. Hence, the importance of the coil, is to bring the temperature of the returning vapour to that

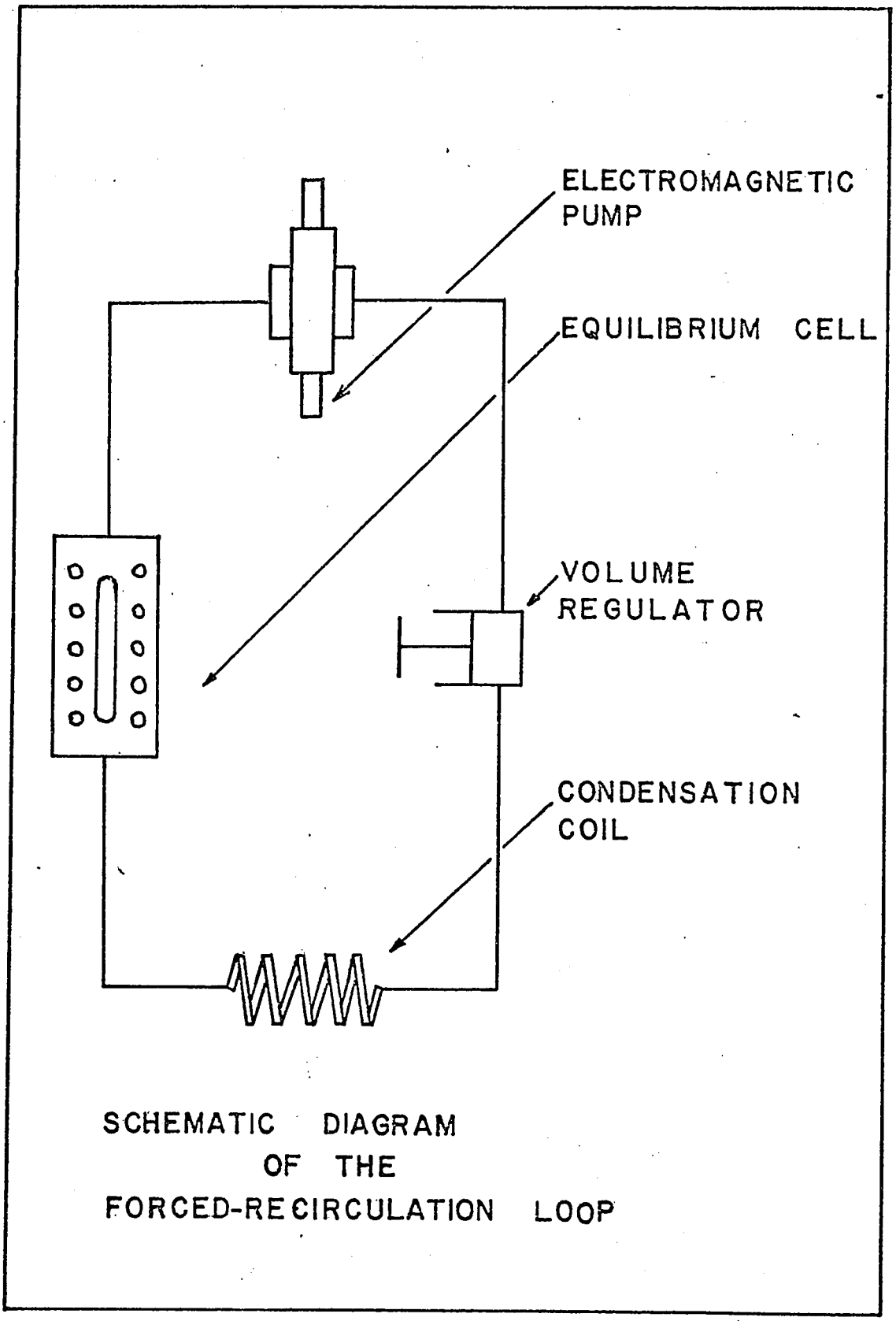
ELECTROMAGNETIC PUMP
EQUILIBRIUM CELL
VOLUME REGULATOR
CONDENSATION COIL
SCHEMATIC DIAGRAM
OF THE
FORCED-RECIRCULATION LOOP

FIGURE (2)

of the cell. In this way, the returning vapour will not alterate the equilibrium position of the vapour-liquid system.

The prime objective of the electromagnetic pump is to recirculate the vapour. It forms a closed system, in that, it is an integral part of the pressurized leak tight system. Pump action permits attainment of equilibrium in a short time due to the mixing effect of the returning vapours as they enter the still from the condensing coil.

The pump is a double-acting piston. It moves to and fro due to the induced magnetic field. Its frequency may be regulated, therefore, regulating the vapour flow rate from 0 to 56 cc. per minute. The developed head is 23 inches of Hg. pressure.

When a vapour sample is withdrawn from the recirculation loop, there is a sudden decrease in system pressure. To re-establish the pressure to normal, a volume regulator is used. By decreasing the volume of the system, the pressure is restored to the equilibrium position. This is necessary to prevent any disturbance in the equilibrium position of the system in case more vapour samples are needed for analysis.

A transparent 100 ml Jerguson gauge was used as the equilibrium cell. The top end of the housing is sealed by a three-way Swagelok connector. Three stainless steel sampling tubes were connected through the connector and extended downwards at different levels into the cell. Also emanating from this connector is the withdrawal vapour-line leading to the electromagnetic pump. The lower end of the cell is welded to an Autoclave joint which links the equilibrium cell to the condensing coil of the returning vapours. A screen is employed to spray and disperse the returning vapours. Another is also located at the exit of the cell to reduce entrainment to a minimum. Two horizontally drilled holes are located 1 1/2 inches from the top and the bottom end of the still housing.

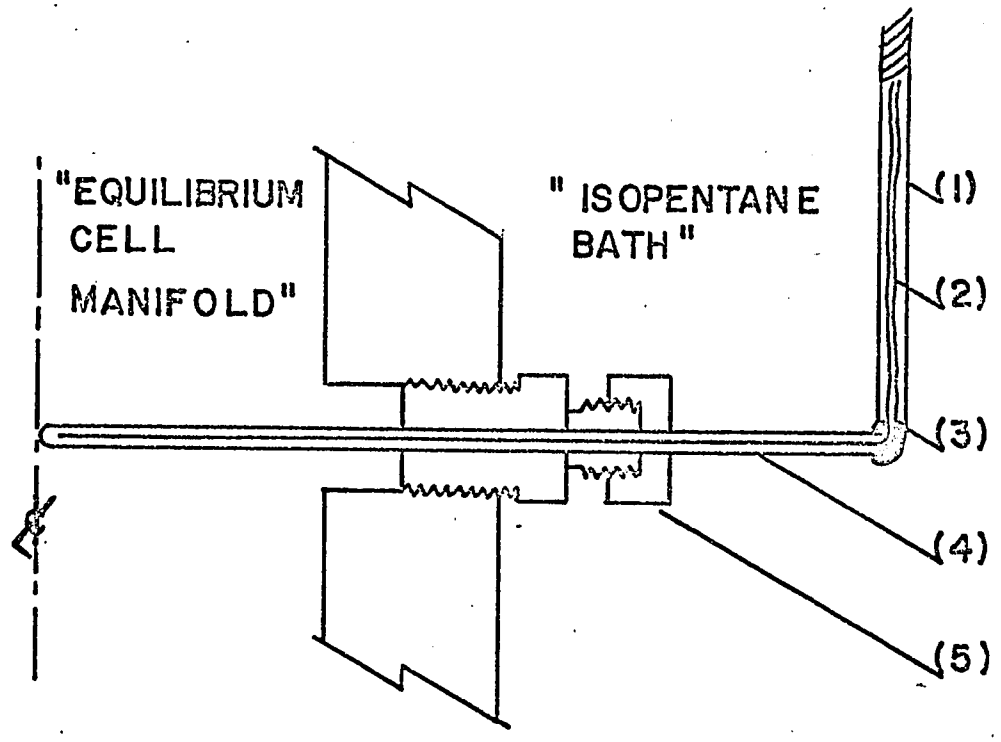

(1) PROTECTIVE TUBING
(2) COPPER CONSTANTAN THERMOCOUPLE
(3) POLYRESIN GLUE
(4) 1/8" OD SS TUBE PACKED WITH ALUMINUM POWDER
(5) 7/16" SS316 COUPLING 'SWAGELOK' TYPE 1/8" ID

SCHEMATIC DIAGRAM
OF THE
THERMOCOUPLE ASSEMBLY

FIGURE (3)

Two laboratory made protective-type copper-constantan thermocouples were each introduced into the cell. The tips of the thermocouples were extended to the center of the cell (Figure (3)).

IV.3 SAMPLING SYSTEM

IV.3-a INTRODUCTION

The gas sampling system is defined as the space where the non-contaminated homogeneous gaseous solution is trapped prior to its analysis. The system is divided into two parts. The gas found in the first section was used to purge the lines leading to the sampling loop exhaust; the second portion, connected to a pressure gauge, contained the source for actual gas samples for analysis.

The forthcoming description will clarify some aspects of the sampling system. A schematic diagram of it is shown in Figure (4).

IV.3-b VALVE FUNCTION

The function of each valve in the sampling system as seen in Figure (4) is briefly described by refering to their assigned numbers.

Valves V_1' and V_2' are leak tight, high pressure valves directly connected to the recirculation loop, while V_1'' and V_2'' are kept partially opened. V_7 isolates the vacuum pump from the sampling system. V_3 and V_5 serve as precautionary measures to protect the sensitive vacuostat and the low pressure gauge when V_4 is open to atmosphere during venting and purging operations. V_6's are used to regulate the flow of gas through the gas chromatograph.

The sample, withdrawn either from the liquid or vapour phase, lies in the space enclosed by $V_1 - V_2 - V_6 - V_7$ and $V_6 - V_3 - V_4 - V_5$. Gas in the former is used to purge the chromatograph lines, in the latter, to take actual gas samples for composition analysis.

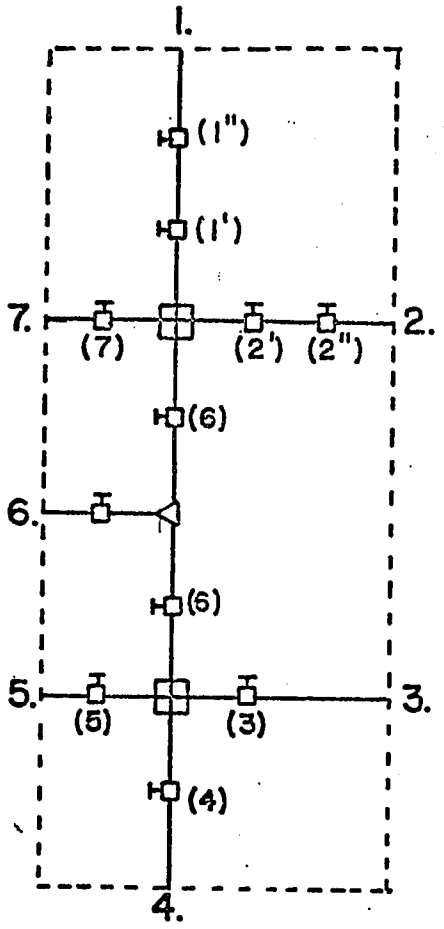

1- VAPOUR SAMPLE INLET
2-LIQUID SAMPLE INLET
3-PRESSURE 0-50 psig
4-ATMOSPHERIC OUTLET or STANDARD MIXT. INLET
5-VACUOSTAT
6-GAS CHROMATOGRAPH INLET
7-VACUUM PUMP
( ) VALVE ASSIGNED NUMBER

SCHEMATIC DIAGRAM OF THE SAMPLING SYSTEM

FIGURE (4)

IV.3-c SAMPLING TECHNIQUE

A general description of the sampling technique is sufficient to understand the knowhow of the actual steps involved in doing analysis. Therefore, an actual detailed procedure involved in pertinent valve operation is omitted.

The sampling system was evacuated to 0.001 mm. of Hg pressure before collecting each sample from the equilibrium system. The reason for this was to prevent contamination of the sample. A total gas pressure of 23 psia was sufficient to provide 4 to 6 gas samples.

The rate at which the gas was introduced into the sampling space from the equilibrium system was measured by a pressure gauge at a rate of about "four pounds per minute". The rate was regulated by two valves in series; the one adjacent to the high pressure side was partially opened, whereas, the other was kept tightly closed. Thus the pressure-rate regulating valve is located adjacently to the sampling system.

Analysis on the liquid phase was first performed. Withdrawal of the liquid phase sample under the foregoing conditions did not cause any detectible changes in system pressure.

The space between the pressure-regulating valves and the equilibrium system was purged prior to composition determination. Hence, the contents from the previous analysis, carried out under different equilibrium conditions, was removed from the static spaces of the recirculation loop. The spaces are located in the liquid sampling probe extending down into the liquid phase and, the vapour sampling outlet line branched closely to the recirculation loop.

Experience have shown that analysis reproducebility in composition was attained when a thirty psia total pressure purge from the liquid

phase was performed. Similarly, a ten psia purge was sufficient from the vapour phase to attain consistency in composition within the experimental error.

The purpose of the following discussion is to show how the samples were systematically analysed for reproducibility, and not for operation of the equipment pertaining to analysis.

To obtain reproducibility in sample composition it was necessary to adopt a vigorous procedure before and during the introduction of the gas partitioner.

The carrier gas flow rate must be maintained constant to that at which the gas chromatograph calibration curve was obtained. A disturbance in flow rate may cause fluctuations in the individually recorded peak heights. In general, peak ratio do not change sensibly.

The operating thermal stabilizer temperature must remain constant at all times. Otherwise, a new calibration curve is needed since it is almost impossible with this stabilizer to return to the original position. Once it was set, the temperature control dial remained in that position as long as the gas partioner was in use for a particular system.

The flow rate of the entering stream into the sampling loop of the automatic sampling valve should be maintained constant. The most important aspect was to close the rate-regulating valve to let the pressure inside the loop equalize that of the surrounding atmosphere. In this way, a constant volume of gaseous solution was introduced each time into the chromatographic column. Moreover, the Gas Sampling Valve provides a convenient and reproducible method for sampling gas stream.

While the above procedures were followed, the recorder base line was adjusted to zero by making proper adjustments. The pertinent details

concerning the operation of the gas chromatograph and its recorder are found in the instructions manual provided for such use.

IV.4 MEASURING AND CONTROL EQUIPMENT

IV.4-a TEMPERATURE REGULATION

Temperature control of the equilibrium cell is extremely important. The temperature of the liquid bath was maintained by a pair of refrigeration coils. They were held vertically on each side of the cell. Liquid nitrogen was used as the refrigerant. The rate of evaporation of liquid nitrogen in the refrigeration coils was controlled by a needle valve and a manometer installed on the exit line of a five-gallon buffer tank located outside the cryostat. The exhaust nitrogen gas was used to cool the electromagnetic pump during operation.

Also located in the cryostat was a resistant type temperature sensing element of a Bayley Temperature Controller Model 250. The sensing probe detects temperature fluctuations about the fixed temperature-range dial position. The control of the bath temperature was achieved by a powerstat adjusted 800-watt immersion heater. The temperature controller can be operated effectively once there is adquate insulation for the cryostat, vigorous and random stirring of the liquid bath and most important, a constant cooling source is imperative. Control specification is to within $\pm$ 0.005°K once all variables have been settled.

IV.4-b TEMPERATURE MEASUREMENT

The temperature of the equilibrium cell was measured by two copper-constantan prptective type thermocouples. One was located in the vapour phase, the other, in the liquid phase.

The reference junction was held at ice-water temperature in a Dewar flask. A Leads and Northrup 7553K-3 Universal Potentiometer was used to detect the junction potential, the smallest division being 1 μv. To balance the potentiometer bridge a Tinsley Galvanometer was used.

The thermocouples were calibrated against the vapour pressure of research grade methane (Appendix I) [21].

IV.4-c PRESSURE MEASUREMENT

Equilibrium pressure of the system was measured by a calibrated Heise Gauge, the pressure range being 0-1000 psia with 1 psia division.

IV.4-d COMPOSITION DETERMINATION

The vapour and liquid compositions were analysed by a Fisher Gas Partitioner model 25V with a built-in sampling valve having one 0.25-ml sample loop. To detect and record the thermistor current, a 1-mv Disc Chart Integrator model 232 was used. The gas samples were swept through the chromatographic columns, hence to the thermal conductivity detectors, by helium gas. Carrier gas flow rate was set to 88 cc/min at a pressure of 20 psig.

Two separating columns are placed in the model 25V. The first, 6 inches long by 0.26 OD has no packing. The second, 6 feet long by 0.25 OD, was packed with 28-30 mesh Silica Gel for the argon-methane system, and 28-30 type 5A Molecular Sieve for the argon-methane-nitrogen system.

The effect of temperature changes on the thermal conductivity cells can be neutralized by using a No. 11-134-250 Thermal Stabilizer. Transfer of heat to the gas partioner will keep the detector well above the highest expected ambient temperature, and hence unaffected by external fluctuations.

Reproducibility in mole fraction is better than 0.005 with the model 25V once all the variables foresaid have been verified before each analysis.

IV.4-e MATERIALS SPECIFICATIONS

Research grade gases were supplied by the Matheson of Canada, Limited, and were used without further purification. Specified minimum purities of the gases are as follows:

GASES	MOLE %
argon	99.995
methane	99.999
nitrogen	99.99

V RESULTS

V.1 TREATMENT OF EXPERIMENTAL OBSERVATIONS

The investigated temperatures with corresponding pressure ranges are listed below.

SYSTEM	TEMPERATURE (°K)	PRESSURE RANGE (psia)	
		$P^s_{CH_4}$	P^s_{Ar}
Ar-CH_4	115.22	19.8	134.22
	123.44	35.5	212.67
	137.07	80.4	405.60
Ar-N_2-CH_4	123.44	35.5	431.5

The experimental observations consists of the peak ratio recorded during analysis of the vapour and liquid phase compositions with corresponding temperature and pressure. Such observations are listed on Tables 6 and 7 of Appendix 111.

A polynomial of the form

$$y = \sum_{i}^{n} a_i x^i$$

was used to represent the calibration curve of mole ratio versus peak ratio. Equations (27, 28, 29, 32, 33) were used to convert the observed peak ratio to mole fractions. The polynomial coefficients are shown in Table 4 of Appendix 11.

The results of such conversion are tabulated in Appendix 1V. Tables 8 and Table 9 represent the P-x-y data for the binary and ternary system respectively.

The observed and recorded pressures were in psia. The liquid and vapour compositions were expressed in mole fraction with respect to argon

for the binary system, and with respect to all components for the ternary system.

The P-x-y and y-x data of the binary and ternary system were plotted on Figures (5) and (6)

The absolute error in the calibration curve is ± 0.006 mole ratio or about ± 0.005 mole fraction. The reproducibility obtained in the calibration was better than ± 0.005 mole fraction and the error in the reported equilibrium compositions is of the same magnetude. In general, the standard deviation in the polynomial representation of the calibration curve is below the figure reported for the absolute error.

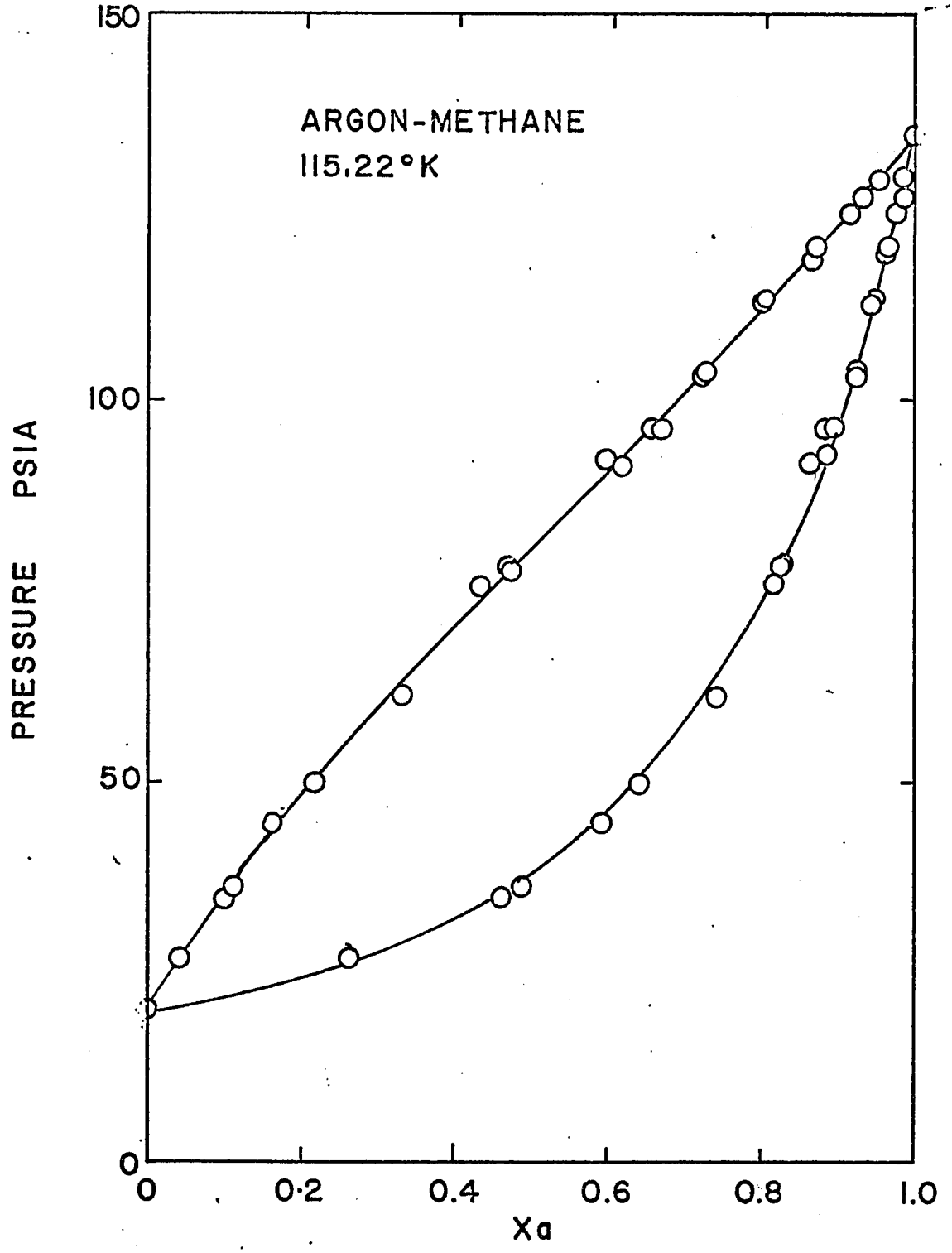

FIGURE (5a): PRESSURE-COMPOSITION DIAGRAM FOR ARGON-METHANE SYSTEM AT 115.22°K

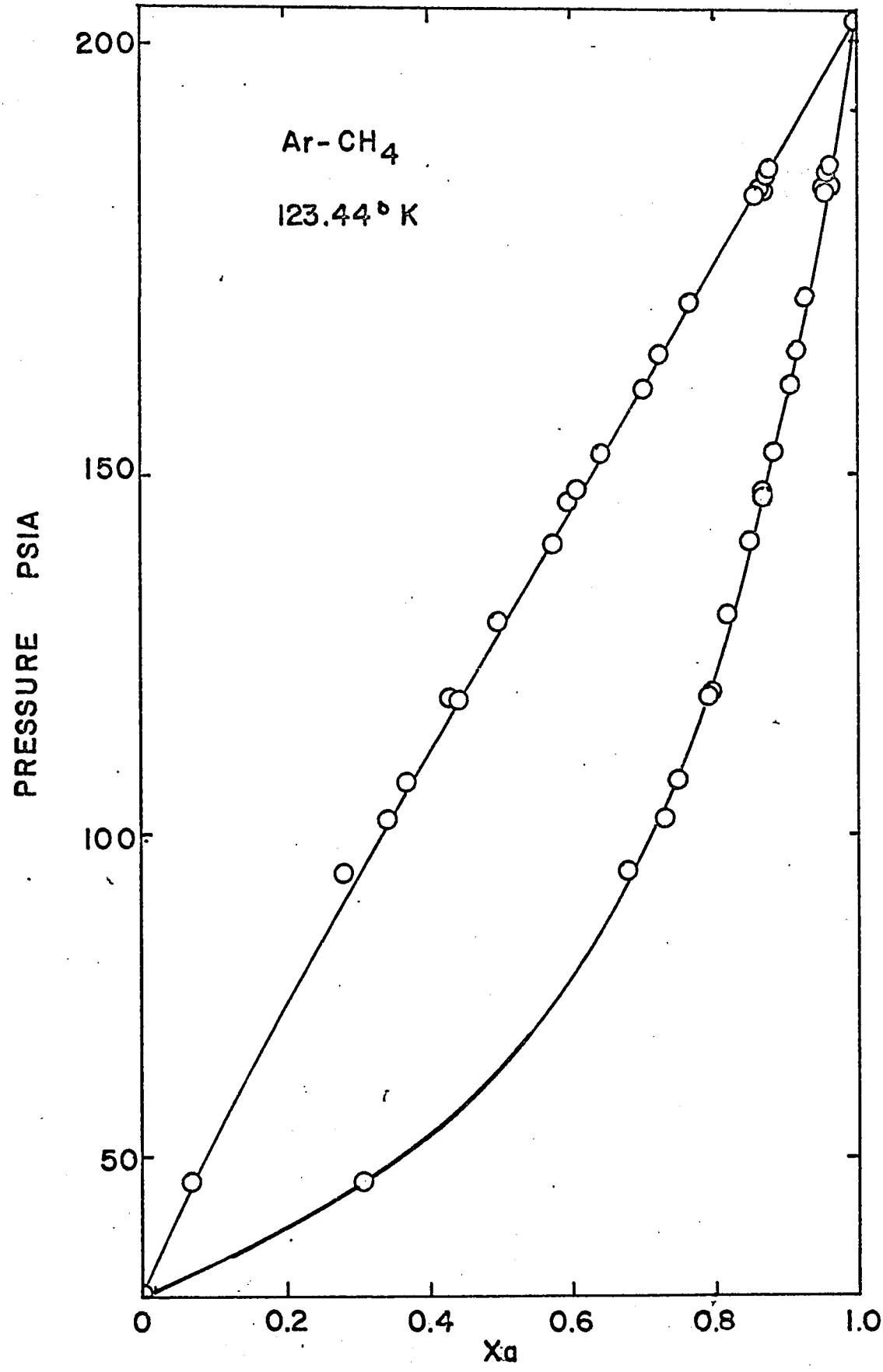

FIGURE (5b): PRESSURE-COMPOSITION DIAGRAM FOR ARGON-METHANE SYSTEM AT 123.44 °K

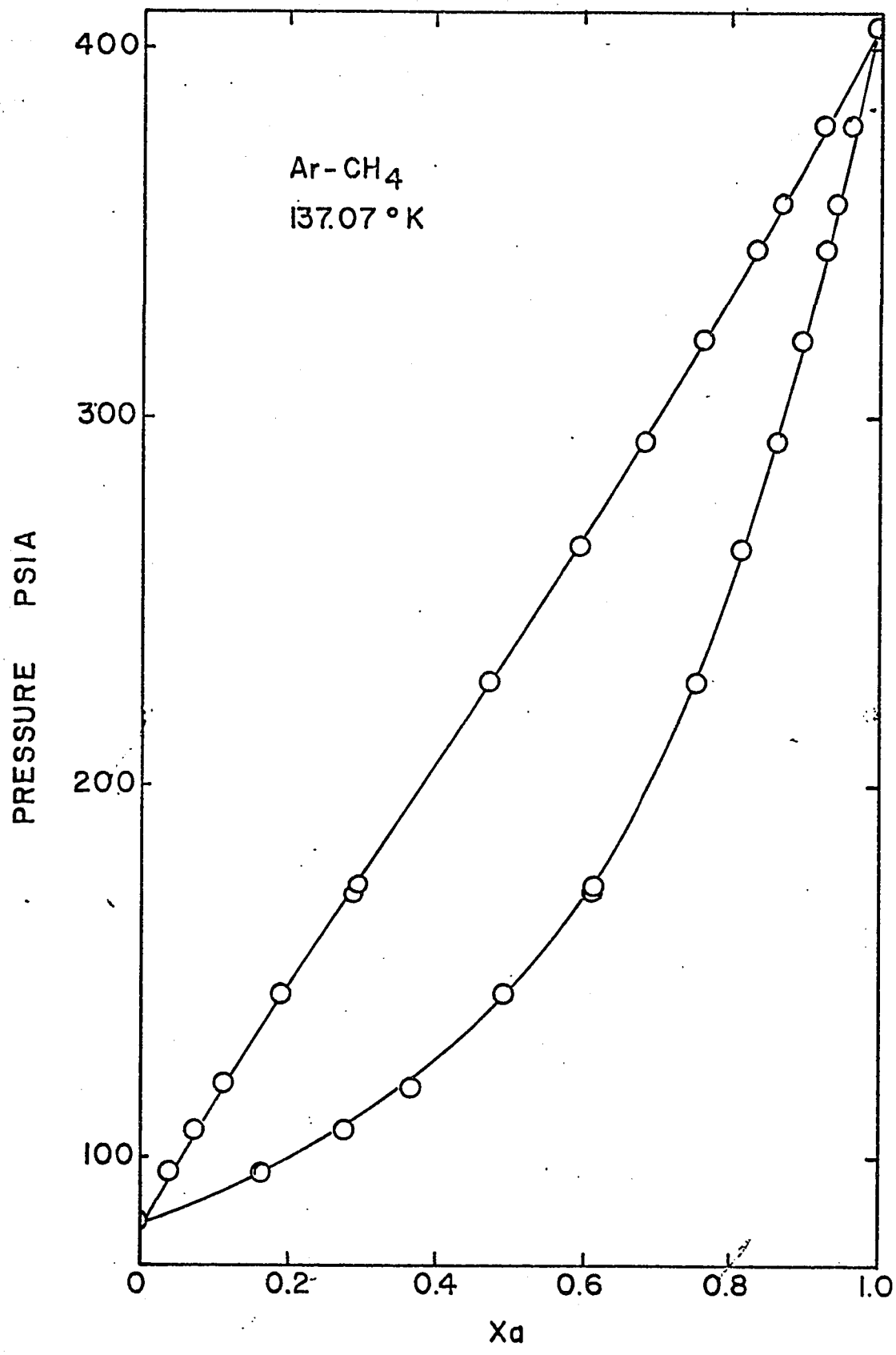

FIGURE (5c): PRESSURE-COMPOSITION DIAGRAM FOR ARGON-METHANE SYSTEM AT 137.07 °K

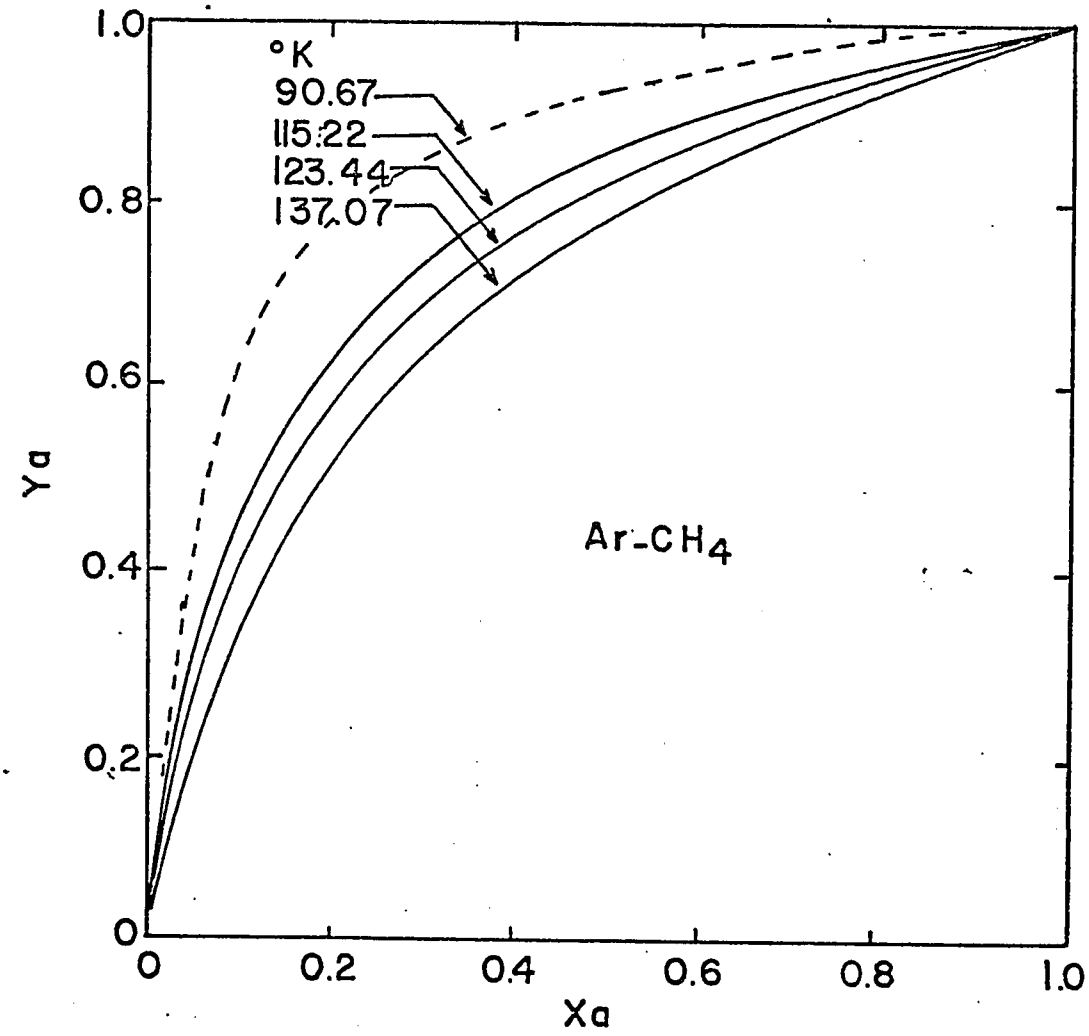

FIGURE (5d): COMPOSITION DIAGRAM FOR ARGON-METHANE SYSTEM

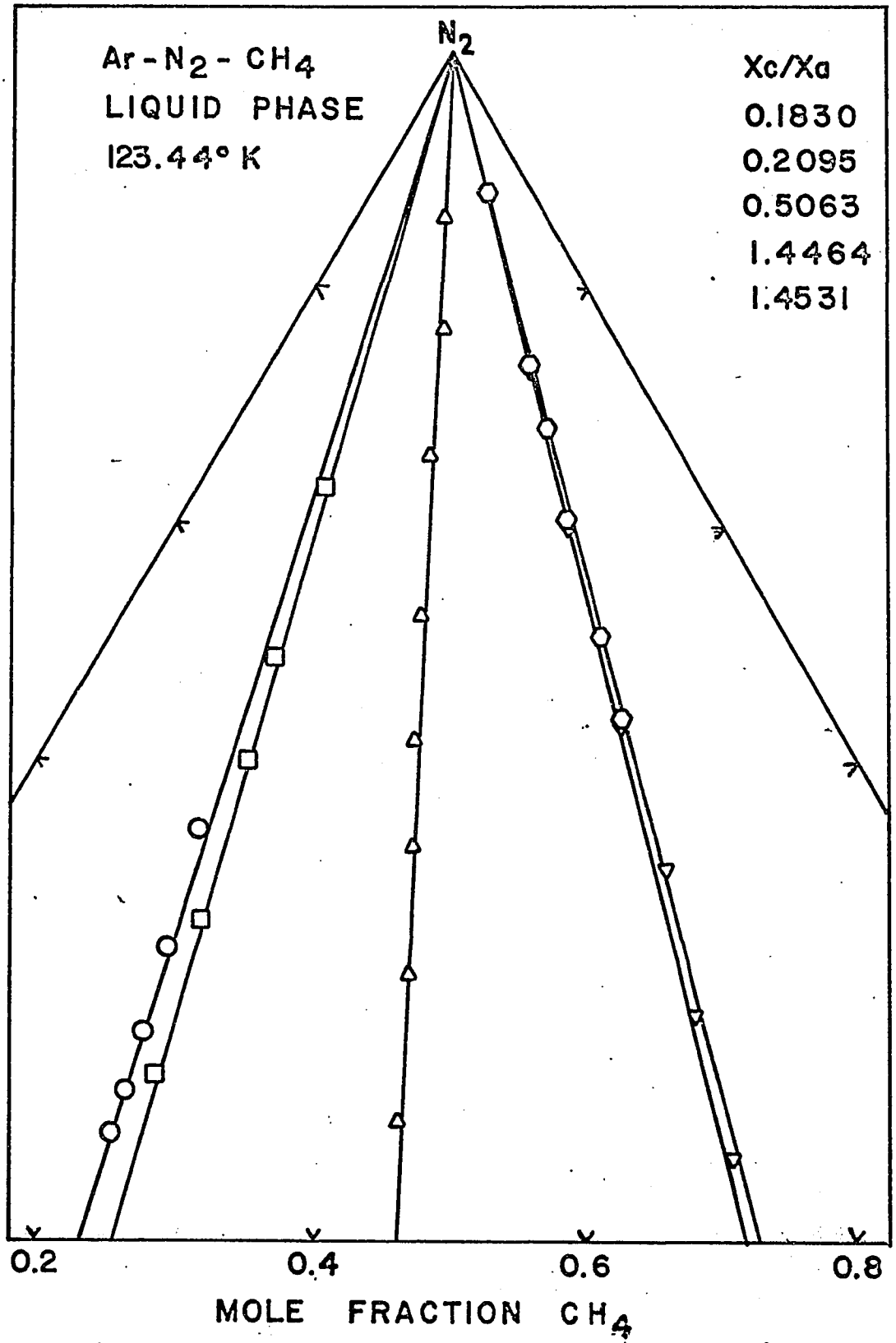

FIGURE (6a): COMPOSITION DIAGRAM OF TERNARY SYSTEM AT 123.44°K (liquid phase)

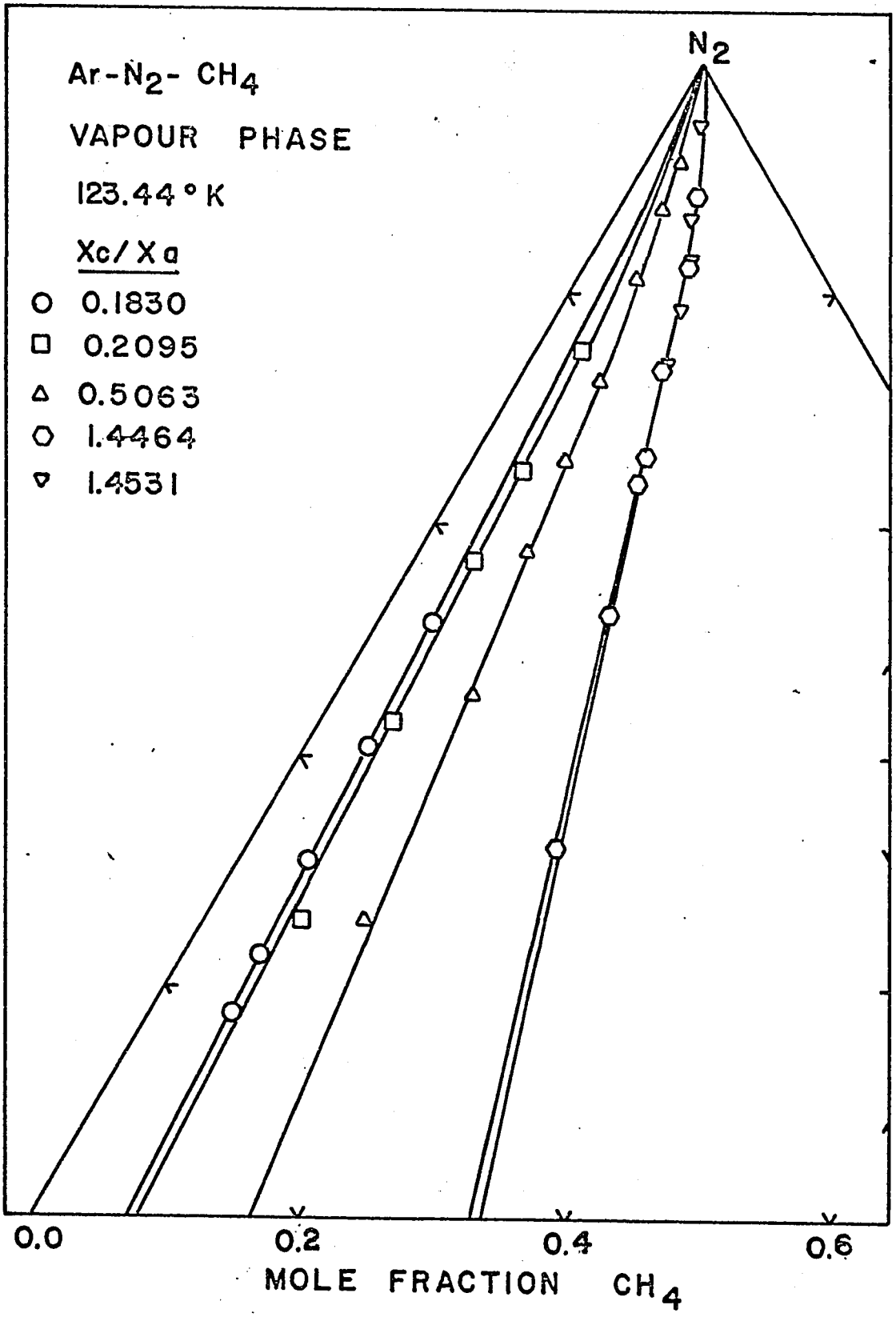

FIGURE (6b): COMPOSITION DIAGRAM OF TERNARY SYSTEM AT 123.44°K (vapour phase)

V.2 CONSISTENCY TEST ON P-x-y EXPERIMENTAL DATA

The general consistency test developped by Chang and Lu [23] was used to verify the consistency of both the binary and ternary P-x-y data. The maximum error in composition was selected as 0.0005 mole fraction and incremented to 0.003 with 0.0005 intervals. The maximum error in pressure and temperature measurements were arbitrarily selected as 0.5 psia and 0.5°K respectively.

The proposed test method of Chang and Lu indicated that some experimental points were non-consistent in the ternary system, however, all points of the binary system were consistent.

The results of such calculations are shown in Table 10 of Appendix V.

VI. DISCUSSIONS

BINARY SYSTEM

VI.1 DETERMINATION OF ACTIVITY COEFFICIENTS

The activity coefficients of the binary system of argon and methane were directly calculated from the experimental data of Tables 8. The methods used to obtain the activity coefficients are briefly reviewed.

At low pressure, the activity coefficients were represented as a function of the second virial coefficients (Equation (2)). The latter were determined by either Prausnitz' correlation [11] or Byrne's [10] experimentally observed second virial coefficients.

At higher pressures, the activity coefficients were estimated from Equation (18) with suitable reference fugacity of the liquid phase reduced to zero pressure. It was evaluated from either Lyckman's correlation of $f^{\bullet}_{i,1}$ given by Equations (12) and (13), or Equation (11) derived from basic principles.

The activity coefficients of Equation (18) in terms of Equation (19) were estimated for a few points at 123.44°K. Thus, the possibility of representing γ by the use of virial coefficients was verified. Also, this would clarify the concept of 'high' or 'moderate' pressures.

The activity coefficients thus obtained were represented by means of the Redlich-Kister equations. The composition dependent activity coefficients were determined for the three isotherms investigated.

Actually, up to 5-term equation parameters were compiled by computer. The parameters of the Redlich- Kister equation shown in Table 11 of Appendix V were those of minimum standard deviation in γ_i.

The results of Table 11 of Appendix V, indicate the activity

coefficients obtained from Equations (11) and (18) gave minimum standard deviation α_{Ar} and α_{CH_4} (Equation (24)) in γ_{Ar} and γ_{CH_4} respectively. Near the freezing point of the heavy component, CH_4, the activity coefficients seem best represented by low pressure Equation (2). As the temperature rises, noticable improvements in representing the activity coefficients by Lyckman's reference fugacity into Equation (18) were observed.

Consistent representation of the activity coefficients was necessary. This was to facilitate the study of all three binary and the ternary isotherms. The latter was studied at a temperature near the critical point of nitrogen. Therefore, Lyckman's correlation of the reference fugacity (Equation (12)), and Equation (18) were reported in the study of this work, however, all correlations were paralleled with those of Equations (11) and (18) [12, 13] which holds for T_r less than 0.91.

Tables 12 of Appendix VI show the observed and calculated values of the log γ_i with corresponding P-x values. Plots of log γ_{Ar} and log γ_{CH_4} versus x_{Ar}, the liquid mole fraction in argon, are shown in Figures(7). The solid line corresponds to the one-suffix Redlich-Kister equation. The activity coefficients of Figures(7)were determined from Lyckman's correlation of the reference fugacity into Equation (18).

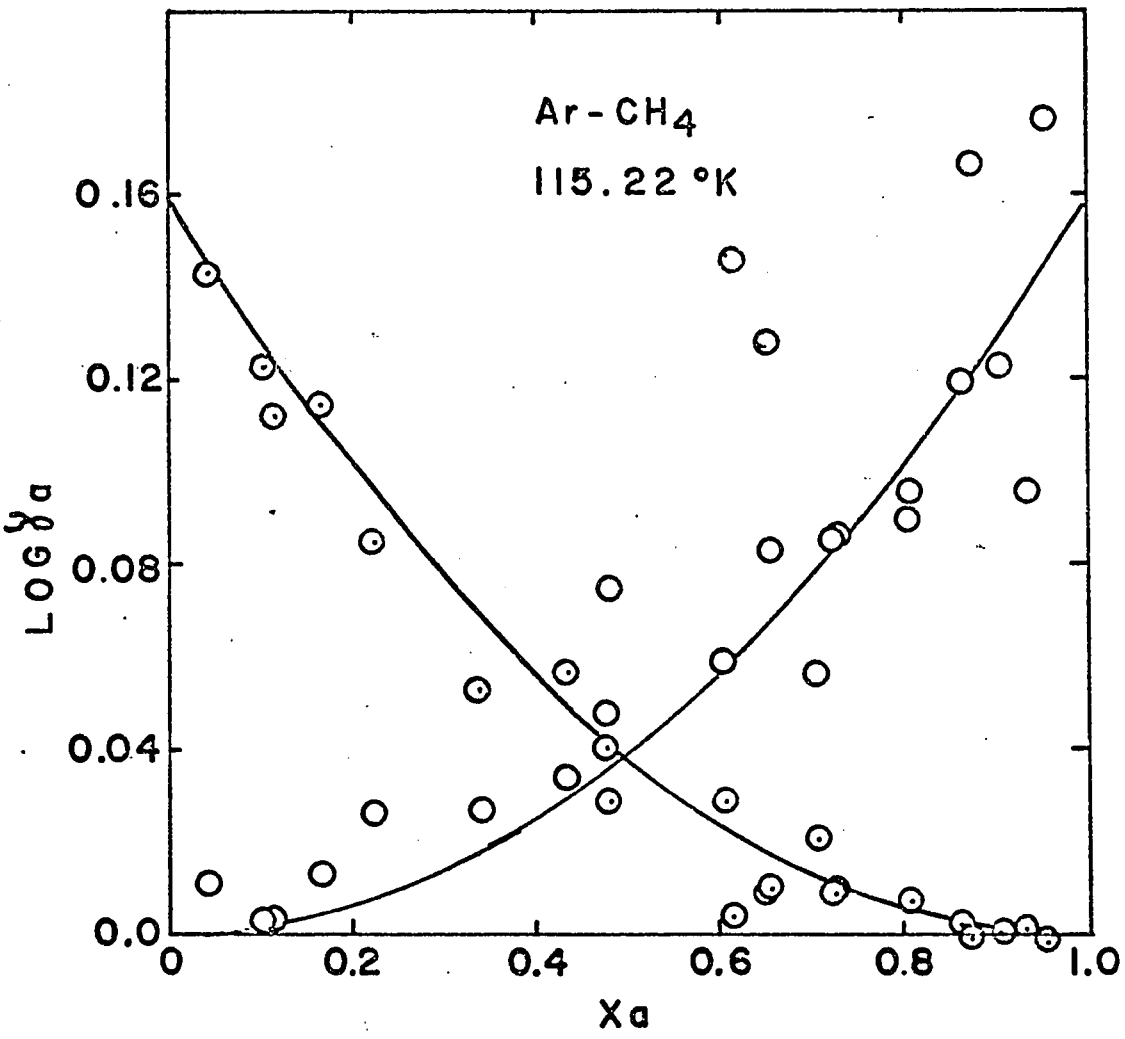

FIGURE (7a): ACTIVITY COEFFICIENT-LIQUID COMPOSITION DIAGRAM FOR $Ar-CH_4$ SYSTEM AT 115.22°K

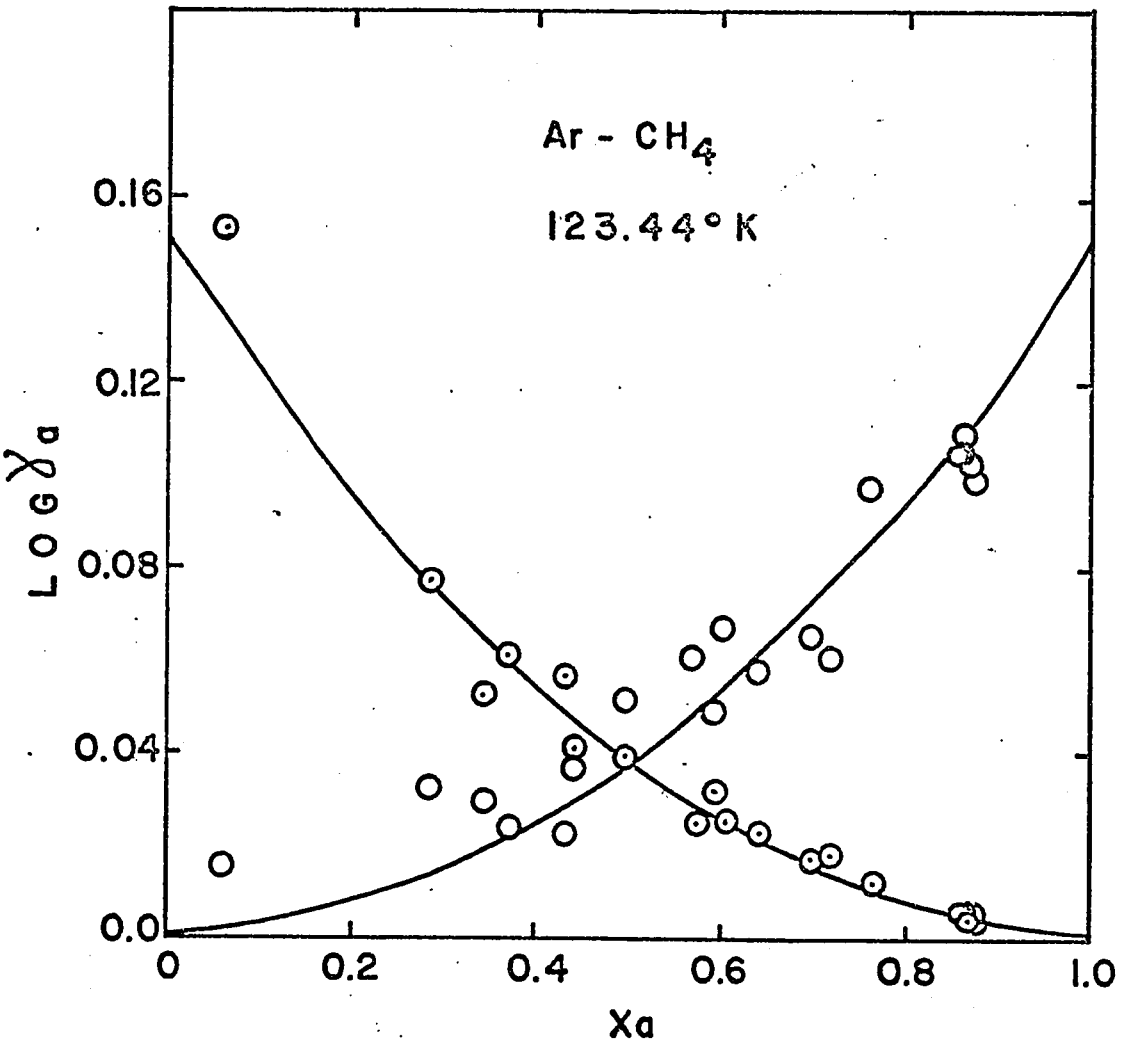

FIGURE (7b): ACTIVITY COEFFICIENT-LIQUID COMPOSITION DIAGRAM FOR $Ar-CH_4$ SYSTEM AT 123.44°K

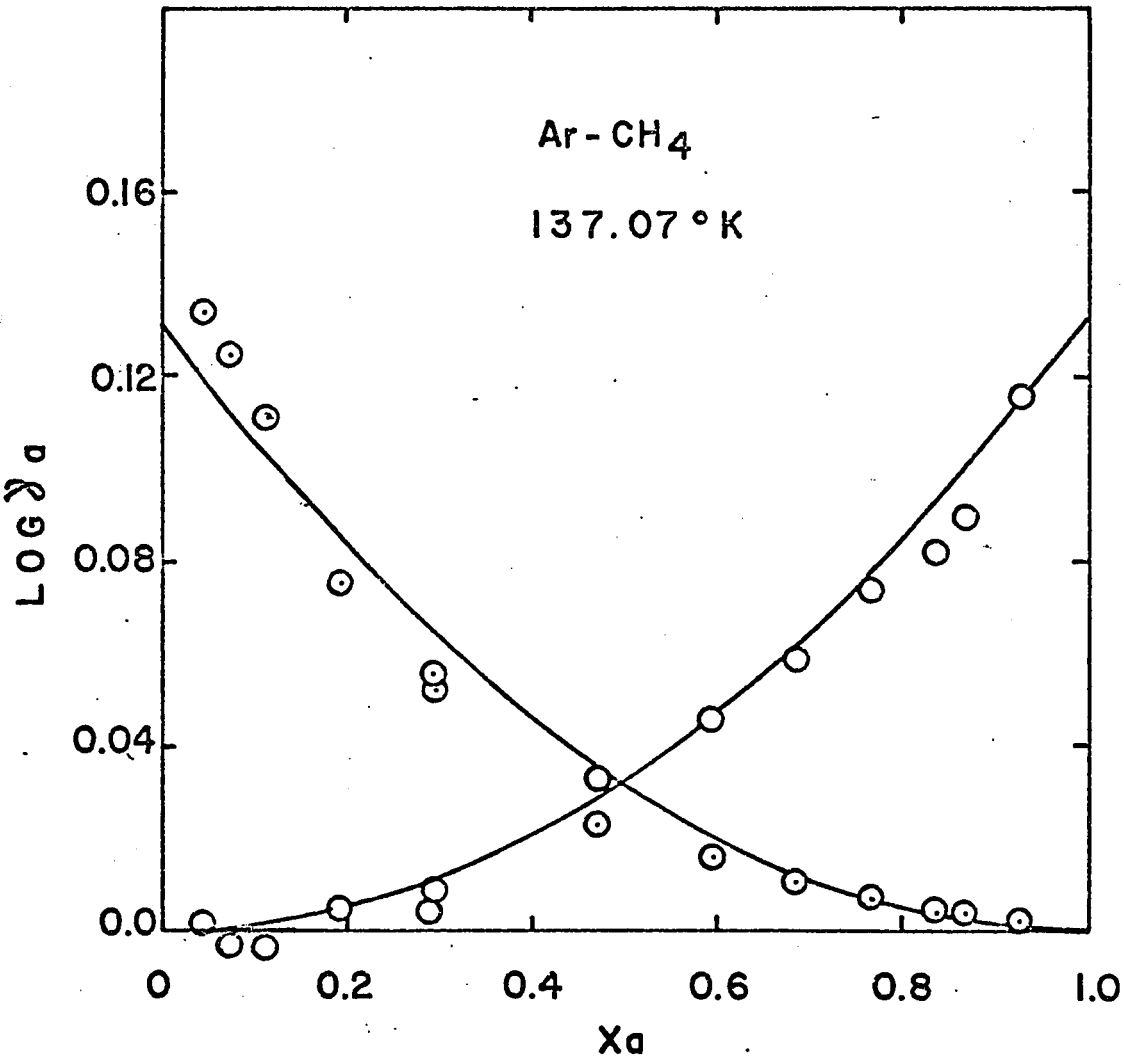

FIGURE (7c): ACTIVITY COEFFICIENT-LIQUID COMPOSITION DIAGRAM FOR $Ar-CH_4$ SYSTEM AT 137.07 °K

VI.2 CORRELATION OF THE LIMITING ACTIVITY COEFFICIENTS

For discussion purposes the following list was prepared in the light of the correlations henceforth discussed.

LIMITING LOG γ_i AT INDICATED TEMPERATURE FROM VARIOUS SOURCES

TEMP. (°K)	PRAUSNITZ'	logP vs $\frac{1}{T}$	CHEUNG'S	MAITRA'S	EQ.(11,18)	EQ.(12,18)
90.67	0.1801		0.227		0.1792	
115.22		0.1545	0.1835		0.1589	0.1707
122.66				0.4015		
123.44		0.1501	0.1715		0.1358	0.1464
132.52				0.0762		
137.07			0.1535		0.1329	0.1344
143.16				0.2349		

The one-term Redlich-Kister parameter is also the limiting value of $\log \gamma_i$ as x_i approaches zero; that is,

$$\lim_{x_j=0} \log \gamma_j = \lim_{x_i=0} \log \gamma_i = B_{ij}$$

To show the dependence of the limiting log γ_i on temperature, a plot of $\underset{x_i=0}{Lt} \log \gamma_i$ versus the reciprocal of the absolute temperature in degree Kelvin was made as illustrated on Figure (8).

The experimental points of Figure (8) pertaining to this work were obtained from Equations (12) and (18) and also Equation (11) with (18) for the calculation of γ and Equations (22) and (23) for the limiting value of log γ_i.

More weight was given to the limiting log γ_i at 137.07°K because the standard deviation in γ_{Ar} and γ_{CH_4} were least when compared against those at 123.44°K and 115.22°K.

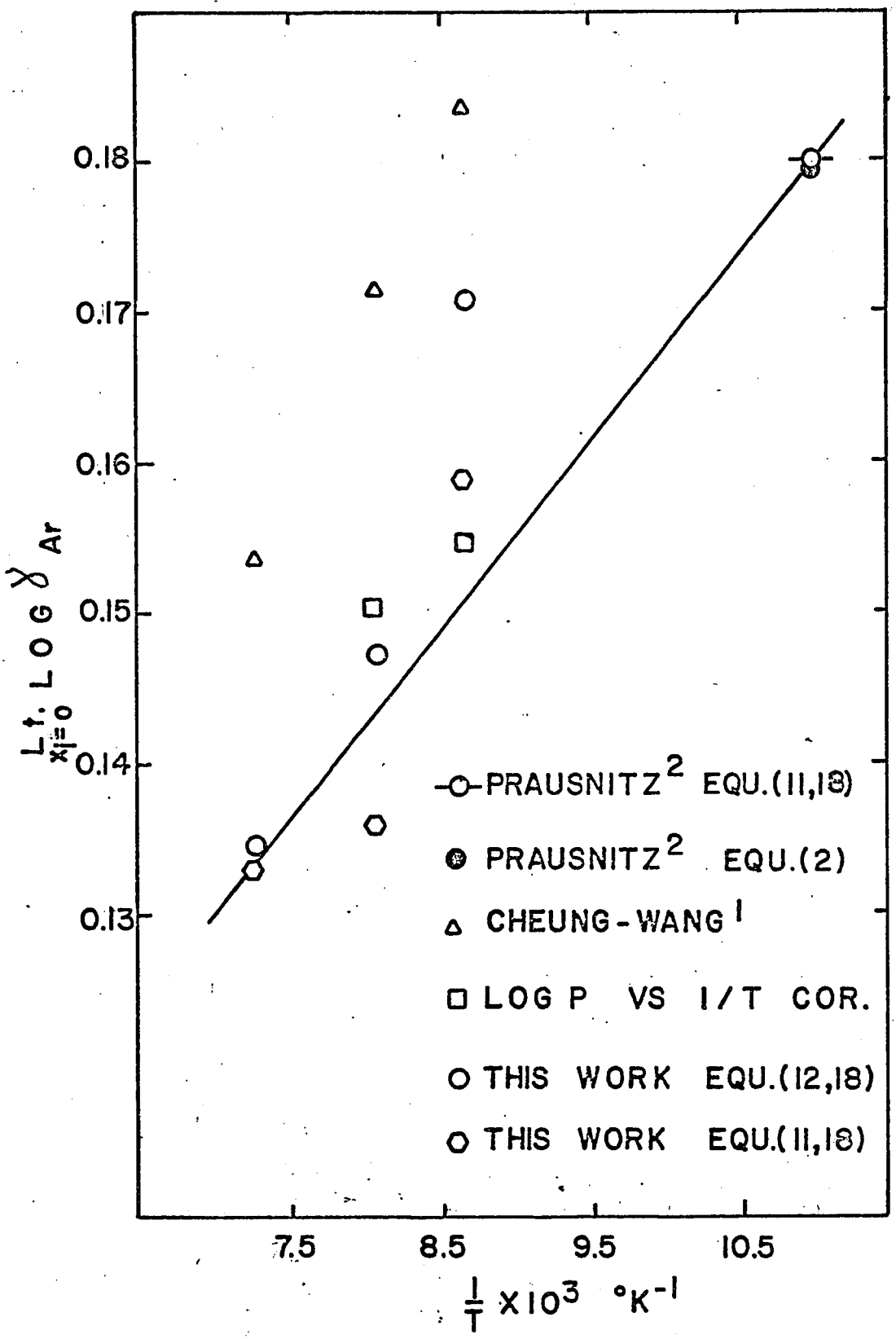

FIGURE (8): LIMITING ACTIVITY COEFFICIENT-TEMPERATURE DIAGRAM FOR Ar-CH_4 SYSTEM

VI.2-a PRAUSNITZ' WORK

Prausnitz' value of the limiting log γ_i at 90.67°K [2] was plotted on Figure(8). To conform with this work, Prausnitz' s reported P-x-y data was processed by Equations (11) and (18) because T_r is less than 0.56. An estimate of the value was also made using low pressure Equation (2): $B_{Ar-CH_4} = 0.1792$, the percent average deviation between both methods being 0.5%.

VI.2-6 LOG P VERSUS 1/T

P-x-y data were first obtained from the smoothed curves of Figures(5) at the three investigated temperatures including the 90.67°K isotherm. Values of pressures and temperature were recorded having vapour and liquid compositions as parameters. A plot of log P vs 1/T was made and the curve was smoothed giving more weight to the points of the 90.67°K and those at 137.07°K.

The P-x-y curves were reconstructed from the smoothed log P vs $\frac{1}{T}$. Consequently, the determination of activity coefficients and evaluation of the Redlich-Kister parameters were made possible. The results have been shown on Figure(8)

VI-2-c CHEUNG AND WANG' S WORK[1]

The infinite dilution activity coefficients have been obtained by correlating experimental data [1] in terms of temperature,

$$\ln \gamma_i = \frac{A_i}{T} (1 - x_i)^2$$

The authors [1] reported the constants A_i of the argon-methane system to be 48.7°K and have indicated that $\gamma^{corr}_{x_i \to 0}$ to be equal to 1.7. However, the calculated $\gamma^{calc}_{x_i \to 0}$ was reported equal to 1.0.

Thus, a correlation with respect to the above equation have indicated

slightly higher infinite dilution activity coefficients, the results of which have been shown in Figure(8)

VI.2-d MAITRA' S WORK

The P-x-y equilibrium data on argon-methane reported by Maitra [5] were processed by Equations (18) and (11) and the Redlich-Kister constants evaluated. The results are shown in the following list:

°K	B_{Ar-CH_4}	%ERROR IN Y
122.6	0.4015	24-30
132.5	0.0762	4-11
143.0	0.2349	12-19

It follows that this data cannot be compared against this work, nor Wang's or Prausnitz' results. Furthermore, the percent deviation in Y exceeds by far the 4% reported in Table 11. The major error encountered in Maitra's work was the fact that he did not have a transparent cell through which the presence of the liquid level could be observed.

TERNARY SYSTEM

VI.3 EXPERIMENTAL y-x CURVES OF THE TERNARY SYSTEM

The vapour-liquid composition of the ternary mixture were investigated using X_c / X_a as parameter. The results of the experimental obsvervations were drawn in Figures(6 a-b).

VI.4 TERNARY EFFECT

VI.4-a BINARY CONSTANTS OF $Ar-N_2$ AND CH_4-N_2 SYSTEM

Adequate and reliable sources were needed to study the possibility of any ternary interaction. Argon-methane data were provided by this work, however, argon-nitrogen and nitrogen-methane data were needed at 123.44°K from other sources.

Wilson's smoothed P-x-y data [27] on argon-nitrogen system was available at 125°K and 122°K. The activity coefficients and the Redlich-Kister constants were determined with 9-40% average deviation in γ_i. The constant $B_{12} = B_{Ar-N_2}$ has been determine on a B versus $\frac{1}{T}$ plot by linear interpolation.

Similarly, Gines smoothed P-x-y data [28] on nitrogen-methane system were available at 122°K and 126.1°K. The average percent deviation in γ was 4-5%.

It must be noted that, in general, minimum standard deviation in γ was recorded for one-suffix equation for the system $Ar-N_2$ and N_2-CH_4.

The values of the constants were determined as: $B_{12} = B_{Ar-N_2} = -0.0490$ (9-40%) and $B_{23} = B_{CH_4-N_2} = 0.3025$ (4-5%).

VI.4-b EVALUATION OF THE TERNARY CONSTANTS C_{123}

The observed activity coefficients of the ternary system were estimated from Lyckman's correlation of the reference fugacity, Equation (12) and Equation (18). The observed excess free energy of Equation (25) was readily estimated. The calculated "Q function" of Equation (26) was obtained through the experimentally determined smoothed values of B_{Ar-CH_4} of Figure (8) The values of the B_{Ar-N_2} and $B_{CH_4-N_2}$ have already been computed and recorded.

With Equations (25) and (26), C_{123} was calculated for each observation. Thus, an average value for C_{123} was obtained, $\overline{C_{123}}$. However, it was shown earlier that not all points of the ternary system were consistent. Therefore, error in composition E(x) was selected as a parameter in the estimation of C_{123}.

In this way, a value of $\overline{C_{123}}$ was determined for consistent points, depending on the parameter E(x). As E(x) increased, the number of consistent points of course increased to a value such that the standard deviation in $\overline{C_{123}}$ was minimum, as shown in Table 13 of Appendix VII.

VI.4-c QUALITATIVE TREATMENT OF C_{123}

A true value of the ternary constant will not be stated as such. Nevertheless, its significance will be discussed in the light of the following arguments.

Carlson, in a personal communication, as reported by Severns [26], concluded that $C_{123} = 0$ was satisfactory for all systems of which the deviations from ideal behaviour were either zero or uniformly positive. In this work, it was observed that the value of $\overline{C_{123}}$ was significantly different from zero. Its value was positive when Υ was calculated from Equation (12) and (18).

A detailed study in the trend of calculated excess free energy was undertaken for a given $\overline{C_{123}}$.

For consistent points when E(x) = 0.0015, there was an indication of a lowering in the calculated excess free energy of Equation (26) when compared to the observed excess free energy of Equation (25). This lowering in excess free energy has been reported by the Severns group [26].

Furthermore, only one ternary system including both positive and negative deviations of the binary pairs have apparently [26]

investigated for which a positive value of C_{123} has been conclusively reported.

A negative C_{123} was reported in the experimental data of the Severns' group. The binary pairs of that mixture were not uniformly positive. The negative sign, although not reported in their conclusions, has been changed by increasing the suffix-equation to a higher order.

The positive sign could also relate the possibility of finding ternary aggregate due to the lowering of the calculated excess free energy.

The ternary constants may not only represent the formation of an aggregation among the constituents but may be a characteristic of temperature. Severns' paper has been relating C_{123} at 323°K, while this work was performed at 123.44°K.

It follows from the forementioned arguments that the possibility of a positive value of C_{123} cannot be entirely rejected, even though the binary pairs of the ternary mixture show uniformly positive deviations from ideality.

CONCLUSIONS

Vapour-liquid equilibrium behaviour for the binary system argon-methane have been investigated at cryogenic temperatures.

The selected temperatures were 115.22, 123.44 and 137.07°K, all of which were below the critical temperatures of the constituents, the ternary system being studied at 123.44°K.

BINARY SYSTEM

Results have been presented in the form of activity coefficients Υ as a function of various concentrations. The Redlich-Kister equations have been used to represent the activity coefficients as a function of liquid mole fraction.

Four methods have been used in calculating the activity coefficients: the basis of selection being minimum standard deviation in Υ when the log Υ-x data were correlated with the Redlich-Kister equations.

Equations (11) and (18) have been found to be the most appropriate form to represent the log Υ versus x curves, for the temperature range 90.67-122.02°K. However, they may be inappropriate to represent Υ near the critical point of the light component (Ar). Then, Lyckman's correlation of the reference fugacity into Equation (18) would be satisfactory for reduced temperature greater than 0.91, but not less than 0.56. Furthermore, calculations of Υ based on low pressure Equation (2) involving the second virial coefficients have been found to be unsatisfactory in representing the high pressure data. Nevertheless, the exact relation of the fugacity coefficient represented by Equation (19) into Equation (18) gave similar values of Υ at 123.44°K. This would indicate that second virial coefficients are sufficient to represent the activity coefficients up to about 212 psia, provided good sources of

virial coefficients are at hand.

Binary constants B_{Ar-CH_4}, for the one-suffix Redlich-Kister equation have been found to satisfactorily represent to within 2.4% in Υ the curves of the observed log Υ versus x at all three isotherms investigated. The constant B_{Ar-CH_4} is the limiting value of the log Υ versus x curves;

$$B_{Ar-CH_4} = \lim_{x_A=0} (\log \Upsilon_A) = \lim_{x_c=0} (\log \Upsilon_c).$$

There has been a definite trend in B_{Ar-CH_4} with temperature as indicated by this work and correlated with Wang's work [1]. However, the latter trend has been found to be slightly higher. Moreover, Maitra's work [5] indicated similar trend, although not so clearly. The higher the temperature, the smaller the value of B_{Ar-CH_4}, inasmuch, the activity coefficients decrease with the increasing temperature.

TEMPERATURE	SMOOTHED B_{Ar-CH_4}	SOURCE
°K	Based on Eq. (12), (18)	
90.67	0.1801	Prausnitz
115.22	0.1520	this work
123.44	0.1440	this work
137.07	0.1329	this work

More specifically, activity coefficients for this system (or organic liquids [29]) having positive deviations from Raoults' Law (Figure 5d) approaches unity as the temperature rises and thus approaches Raoult's Law.

To give an idea of the order of magnetude of the change in the activity coefficients, a change of 5 percent in the activity coefficient

results from a 8°K temperature change. The average percent deviation range in the fitting of the log Υ versus x curves have been found to be 2% which is far better than what reported by Wang [1] and lies within the maximum possible experimental error in composition determination and calibration. (Appendix 11)

TERNARY SYSTEM

Mixtures having uniformly positive deviations from ideality in the binary pairs may not necessarily be represented by $C_{123} = 0$. The system argon-nitrogen-methane has been found to require a value of C_{123} that was significantly greater than zero. The justification in accepting such a value has been based on the lowering of the calculated excess free energy which would account for the possible interaction among the constituents of a ternary mixture.

Since not enough work has been done pertaining to this aspect, it was difficult to support a possible trend of C_{123} with temperature and/or with the features of the binary pairs, that is, uniform or non-uniform behaviour in their deviations from ideality.

Also, as noted in Table 13 of Appendix VII, when the Redlich-Kister suffixed equation is increased to two terms, the value of the ternary constant is decreased towards zero. However, it is not advised [25] to use higher suffixed equations exept for extremely complex systems with highly accurate data. Furthermore, sources for the binary pairs constituting the the ternary system were scarce and not of fine caliber.

VIII BIBLIOGRAPHY

(1) Cheung, H. and Wang, D.I.-J., I/EC, 3, 255 (1964).

(2) Sprow, F.B. and Prausnitz, J.M., A.I.Ch.E. Jl., 12, 780 (1966).

(3) Sprow, F.B. and Prausnitz, J.M., Cryogenics, Dec., 358 (1966).

(4) Pool, R.A.H., et.al., Trans. Faraday Soc., 58, 1692 (1962).

(5) Maitra, K.K., M.Sc. Thesis, Chem. Eng. Dept., U. of O. (1966).

(6) Chang, S.-D., M.Sc. Thesis, Chem. Eng. Dept., U. of O. (1967).

(7) Chang, S.-D. and Lu, B.C.-Y., Chem. Engng. Prog. Symp. Ser., 63, 18 (1967).

(8) Zelfde, P. van't, et.al., Physica, 28, 241 (1968).

(9) Van Ness, H.C., 'CLASSICAL THERMODYNAMICS OF NON-ELECTROLYTE SOLUTIONS' , MacMillan, N.Y. (1964). pp 121.126,159,39.

(10) Byrne, M.A., et.al., Trans. Faraday Soc., 64, 1733 (1968).

(11) Prausnitz, J.M., A.I.Ch.E. Jl., 5, 4 (1959).

(12) Chueh, P.L. and Prausnitz, J.M., A.I.Ch.E. Jl., 13, 1103 (1967).

(13) Chueh, P.L. and Prausnitz, J.M., A.I.Ch.E. Jl., 13, 1099 (1967).

(14) Prausnitz, J.M. and Gunn, R.D., A.I.Ch.E. Jl., 4, 430 (1958).

(15) Prausnitz, J.M., A.I.Ch.E. Jl., 5, 3 (1953).

(16) Chueh, P.L. and Prausnitz, J.M., I/EC Fund., 4, 492 (1967).

(17) Chao, K.C. and Seader, J.D., A.I.Ch.E. Jl., 7, 598 (1961).

(18) Lyckman, E.W., et.al., Chem. Engng. Sc., 20, 685 (1965).

(19) Pitzer, K.S., et.al., J. Am. Chem. Soc., 77, 3427,3433 (1955).

(20) Lewis, G.N., et.al., 'THERMODYNAMICS' , 2nd ed., McGraw-Hill, N.Y. (1961), p 605.

(21) Itterbeek, V., et.al., Physica, 30, 1896 (1964).

(22) Itterbeek, V., et.al., Physica, 30, 2119 (1964).

(23) Chang, S.-D. and Lu, B.C.-Y., Paper presented and accepted for publication in The International Symposium on Distilation, Brighton, England, Sept. 1969.

(24) Din, F., 'THE THERMODYNAMIC FUNCTION OF GASES', Butterworth, London (1956).

(25) Redlich. O. and Kister, A.T., I/EC, 40, 345 (1948).

(26) Severns, W.H., et.al., A.I.Ch.E. Jl., 1, 401 (1955).

(27) Wilson, G.M., et.al., Technical Documentary Report No. APLTDR 64-64, April (1964).

(28) Cines, M.R., et.al., Chem. Eng. Progr. Symp. Ser., No. 6 49, 1 (1953).

(29) Carlson, H.C. and Colburn, A.P., I/EC, 34, 581, No. 5.

(30) Ruheman, M. and Harmens, A., The Chemical Engineer, Series No. 4, 254 (1967).

(31) Hala, E., Pick, J. and Vilim, O., 'VAPOR-LIQUID EQUILIBRIUM ', 2nd Ed., Permagon Press (1967), Chap. 4.

(32) Redlich, O. and Kwong, J.N.S., Chem. Rev., 44, 233 (1949).

(33) Chueh, P.L. and Prausnitz, J.M., A.I.Ch.E. Jl., 13, 896 (1967).

(34) Michels, A., et.al., Physica, XXIV, 659 (1958).

APPENDIX 1

THERMOCOUPLE CALIBRATION

Research grade methane was used in the calibration of the thermocouples. By experience, it was found that a calibration of the desired temperature had to be done prior to each isotherm run as a routine check. An approximate temperature in the region of investigation was first chosen with its corresponding vapour pressure. The temperature of the cryostat was adjusted so that the selected vapour pressure of methane was obtained by directly reading the absolute pressure gauge. The vapour was recirculated for an hour. At equilibrium, (temperature constant and pump shut off) the exact pressure was recorded along with the potentiometer voltage reading. Consequently, before each isothermal study, the temperature was set exactly at the calibration point and the corresponding pressure of pure methane was verified for agreement with the original calibration.

The temperature was obtained by interpolation from vapour pressure data of methane [21]. The prediction of the vapour pressure of argon was performed by interpolation of argon vapour pressure data [22].

It should be noted that; for example, at 35.5 psia methane pressure, the difference in vapour and liquid temperature at equilibrium conditions was negligible. A 0.05 microvolt (1°K=21μv) potentiometer reading gives a temperature difference of about 0.0002°K.

Table 1 gives the necessary numerical information as to the calibration of the thermocouples.

TABLE 1

CALIBRATION OF VAPOUR-LIQUID LOCATED COPPER-CONSTANTAN THERMOCOUPLE

OBSERVED METHANE V.P. (PSIA)	POTENTIOMETER READING (mv) THERMOCOUPLE LOCATED IN THE LIQUID PHASE	POTENTIOMETER READING (mv) THERMOCOUPLE LOCATED IN THE LIQUID PHASE	TEMPERATURE REF.(21) °K (± 0.01)	ARGON VAPOUR PRESSURE PREDICTED PSIA REF.(22)	ARGON VAPOUR PRESSURE OBSERVED PSIA
19.8	4.8120	4.8114	115.22	134.66	134.22
35.5	4.6338	4.6333	123.44	213.88	212.67
80.4	4.3183	4.3179	137.07	405.84	405.60

APPENDIX 11

GAS CHROMATOGRAPH CALIBRATION

The calibration of the gas partitioner was made against prepared binary mixtures of known compositions. The calibration data for the binary system are shown in Table 2 as argon to methane peak ratio P_a / P_c, and argon to methane mole ratio, x_a / x_c.

The peak ratio superscripts, ', '', ''', denote the sensitivity range used on the gas chromatograph. A low concentration of a component requires a high sensitivity for detection. Actually, 2 and 10 per cent sensitivity were sufficient to record the entire range of composition investigated for all three isotherms.

The calibration data for each sensitivity range was least-square fitted by one to five degree polynomials.

It was found, for all ranges of sensitivity, that a fourth degree polynomial indicated the minimun standard deviation in mole ratio. For binary mixture analysis, either from liquid or vapour phase, the following equations were used depending on the sensitivity range used:

$$MR' = \sum_{i}^{4} A_i \, (PR')^i \qquad 27a$$

$$MR'' = \sum_{i}^{4} B_i \, (PR'')^i \qquad 28a$$

$$MR''' = \sum_{i}^{4} C_i \, (PR''')^i \qquad 29a$$

for $Pr < 1.0$, and

$$MR' = \sum_{i}^{4} D_i \, (PR')^i \qquad 27b$$

$$MR'' = \sum_{i}^{4} E_i \, (PR'')^i \qquad 28b$$

$$MR''' = \sum_{i}^{4} F_i \, (PR''')^i \qquad 29b$$

for $PR \geq 1.0$. The polynomial coefficients are shown Table 4. $PR = P_a / P_c$, the superscripts being omitted, and $MR = x_a / x_c$ (or $MR = y_a / y_c$) depending on the case. The liquid mole fraction of methane and argon is estimated from Equations (27), (28), (29) by

$$x_a = \frac{x_a / x_c}{1 + x_a / x_c} \text{ and } x_c = \frac{1}{1 + \frac{x_a}{x_c}} \qquad 30,31$$

Similar expressions for y_a and y_c may be obtained.

In a similar way, calibration data for ternary mixtures were obtained by analysing two binary gaseous solutions having argon as the common component. Table 3 shows the calibration results in terms of P_c / P_a and P_n / P_a with respective x_c / x_a and x_n / x_a. The subscript n refers to the nitrogen component. The gas partitioner was set at 2 per cent full scale sensitivity. This was sufficient to analyse the entire composition range of the ternary system.

For the same reason as discussed in the binary calibration section, a fourth-degree polynomial was used to fit the calibration data:

$$MR_{ca} = \sum_{i}^{4} G_i \, (PR_{ca})^i \qquad 32a$$

$$MR_{na} = \sum_{i}^{4} H_i \, (PR_{na})^i \qquad 33a$$

for $PR < 1.0$, and,

$$MR_{ca} = \sum_{i}^{4} I_i \, (PR_{ca})^i \qquad 32b$$

$$MR_{an} = \sum_{i}^{4} J_i \, (PR_{an})^i \qquad 33b$$

for $PR \geqslant 1.0$. The polynomial coefficients are shown on Table 4.

$PR_{ca} = P_c / P_a$ and $PR_{na} = P_n / P_a$ and MR_{ca} and MR_{na} represent for either liquid or vapour analysis, methane to argon mole ratio and nitrogen to argon mole ratio, respectivily.

It must be noted that when $PR \geqslant 1.0$, $PR = \frac{1}{PR}$ and $MR = \frac{1}{MR}$.

It is possible to show that the mole fraction can be represented by the following equations:

$$x_a = \frac{1}{1 + PR_{ca} + PR_{na}} \quad , \qquad (34)$$

$$x_c = \frac{PR_{ca}}{1 + PR_{ca} + PR_{na}} \quad , \qquad (35)$$

and

$$x_n = \frac{PR_{na}}{1 + PR_{ca} + PR_{na}} \quad . \qquad (36)$$

Table 5 shows the deviation encountered in polynomials representing mole ratio of various systems for Equations (27), (28), (29), (32), (33) in mole ratio determination.

TABLE 2

ARGON-METHANE CALIBRATION DATA

SENSITIVITY(')		SENSITIVITY('')		SENSITIVITY(''')	
P_a / P_c	x_a / x_c	P_a / P_c	x_a / x_c	P_a / P_c	x_a / x_c
0.7027	0.0758	0.2775	0.8181	0.1302	0.0758
1.0486	0.1111	0.3438	1.0000	0.1953	0.1110
1.0859	0.1129	0.5167	1.5000	0.4455	0.2500
2.2361	0.2500	0.5192	1.5125	0.7561	0.4286
2.2885	0.2500	0.7989	2.3333	0.7682	0.4336
3.8470	0.4286	0.7807	2.3444	0.9551	0.5408
3.9895	0.4336	1.3532	3.9875	1.1613	0.6667
4.8246	0.5408	1.3750	4.0504	1.1537	0.6708
		3.0740	8.9010	1.3998	0.8181
		5.4670	17.5529	1.7627	1.0000
		5.6590	17.0505	1.7390	1.0000
		7.6050	22.3714	2.6184	1.5000
		10.1833	27.8184	2.6718	1.5125
		9.7319	30.5457	4.0195	2.3444
				7.1815	4.0504

TABLE 3

ARGON(a)-NITROGEN(n)-METHANE(c) CALIBRATION DATA

P_c / P_a	x_c / x_a	P_n / P_a	x_n / x_a
0.2631	0.4306	0.2134	0.2541
0.4040	0.6725	0.3618	0.4399
0.5821	1.0040	0.5490	0.6734
0.8562	1.4969	0.7944	1.0072
1.3154	2.3647	1.1604	1.5031
2.2241	4.1151	1.8298	2.4305
		2.9878	4.1099

TABLE 4

POLYNOMIAL COEFFICIENTS OF CALIBRATION CURVES

DEGREE i=	1	2	3	4
COEFFICIENTS				
A	0.0942	0.0166	-0.0055	0.0006
B	0.5910	-0.0260	0.0095	-0.0009
C	3.0970	-0.1569	0.0427	-0.0029
D	9.2222	-1.7170	3.9949	-1.9429
E	1.7044	0.0633	-0.0147	0.0009
F	0.3368	-0.0025	0.0053	-0.0012
G	1.1433	0.2118	-0.0852	0.0135
H	1.5595	0.3490	-0.1713	0.0329
I	0.6886	0.1279	-0.0407	0.0043
J	0.5512	-0.0105	0.0250	-0.0048

TABLE 5

STANDARD DEVIATION IN CALIBRATION POLYNOMIALS

SYSTEM	EQUATION NUMBER	SENSITIVITY	STANDARD DEVIATION
Ar/CH_4	21a	(')	0.0049
Ar/CH_4	22a	('')	0.0120
Ar/CH_4	23a	(''')	0.0102
CH_4/Ar	21b	(')	0.0049
CH_4/Ar	22a	('')	0.0056
CH_4/Ar	23b	(''')	0.0092
CH_4/Ar	26a	('')	0.0071
N_2/Ar	27a	('')	0.0049
Ar/CH_4	26b	('')	0.0080
Ar/N_2	27b	('')	0.0037

APPENDIX 111

EXPERIMENTAL OBSERVATIONS

The experimental observations are, in fact, the peak ratio recorded from the analysis of the vapour phase and liquid phase samples, with corresponding equilibrium pressure. Three binary and one ternary isotherm were studied.

In the argon-methane system; the pressure P, liquid argon to methane peak ratio $(P_a / P_c)_L$ and vapour argon to methane peak ratio $(P_a / P_c)_V$ with corresponding sensitivity (', '', ''') as denoted in Appendix II, are shown in Table 6(a, b, c).

For the ternary system of argon-methane-nitrogen; the pressure P, the liquid nitrogen to argon peak ratio, $(P_n / P_a)_L$, the liquid methane to argon peak ratio, $(P_c / P_a)_L$, and similarly from the vapour analysis, $(P_n / P_a)_V$ and $(P_c / P_a)_V$ are collected in Table 7.

TABLE 6a

BINARY EXPERIMENTAL OBSERVATIONS

TEMPERATURE 115.22 °K

PRESSURE	$(P_a / P_c)_L$	$(P_a / P_c)_V$
26.8	0.4573 '	0.6201 ''
34.8	1.1149 '	1.5356 ''
36.0	1.2461 '	1.6894 ''
44.0	1.8671 '	2.5222 ''
49.6	2.5596 '	3.1581 ''
61.0	0.8674 ''	1.0012 '''
75.0	1.3449 ''	1.5155 '''
77.7	1.6087 ''	1.5476 '''
78.0	1.5781 ''	1.6576 '''
91.0	0.5286 '''	2.1196 '''
92.0	2.6057 ''	2.5858 '''
95.6	0.6387 '''	2.9099 '''
96.0	0.6326 '''	2.6503 '''
102.9	0.8796 '''	4.0050 '''
103.5	0.8107 '''	4.0654 '''
103.9	0.9012 '''	4.0943 '''
112.0	1.3653 '''	6.0511 '''
112.9	1.4087 '''	6.1526 '''
118.0	2.0859 '''	8.5081 '''
119.6	2.3681 '''	8.5936 '''
124.2	3.6452 '''	14.6416 '''
126.0	4.5613 '''	19.4228 '''
128.3	6.8459 '''	24.0721 '''

TABLE 6b

BINARY EXPERIMENTAL OBSERVATIONS

TEMPERATURE 123.44 °K

PRESSURE	$(P_a / P_c)_L$	$(P_a / P_c)_V$
51.0	0.6441 '	3.9034 '
94.0	3.6731 '	0.6955 '''
101.1	0.9353 ''	0.8722 '''
106.9	1.0368 ''	1.0013 '''
118.5	1.3336 ''	1.2749 '''
118.0	1.4092 ''	1.2562 '''
129.0	0.3284 '''	1.4804 '''
139.5	0.4469 '''	1.8852 '''
145.8	0.4925 '''	2.1551 '''
146.5	0.5138 '''	2.1206 '''
152.0	0.6012 '''	2.4984 '''
161.0	0.7836 '''	3.1216 '''
166.0	0.8783 '''	3.5251 '''
173.5	1.1213 '''	4.0077 '''
188.0	2.0338 '''	7.0143 '''
189.0	2.1944 '''	7.4603 '''
189.0	2.0959 '''	7.2150 '''
190.5	2.3327 '''	8.0568 '''
191.5	2.4479 '''	8.5540 '''

TABLE 6c

BINARY EXPERIMENTAL OBSERVATIONS

TEMPERATURE 137.07 °K

PRESSURE	$(P_a / P_c)_L$	$(P_a / P_c)_V$
95.4	0.4194 '	1.8661 '
107.0	0.7851 '	0.6762 ''
119.5	1.2090 '	1.0336 ''
144.0	2.1892 '	1.7172 ''
172.8	0.7248 ''	2.7363 ''
172.0	0.7141 ''	0.5268 '''
227.5	1.5448 ''	1.0224 '''
264.8	2.5554 ''	1.5290 '''
293.4	0.7239 '''	2.0983 '''
321.4	1.1189 '''	3.0068 '''
345.6	1.7164 '''	4.4538 '''
358.0	2.2455 '''	5.6759 '''
378.4	4.2714 '''	9.9919 '''

TABLE 7

TERNARY EXPERIMENTAL OBSERVATIONS

TEMPERATURE :123.44 °K

x_c/x_a	P(psia)	$(P_n/P_a)_L$	$(P_c/P_a)_L$	$(P_n/P_a)_V$	$(P_c/P_a)_V$
0.1830	191.3	0.1067	0.1849	0.1941	0.0516
	200.0	0.1523	0.1851	0.2694	0.0523
	212.7	0.2287	0.1856	0.3979	0.0504
	231.9	0.3534	0.1811	0.6009	0.0545
	255.0	0.5515	0.1815	0.9000	0.0603
0.2095	202.2	0.1818	0.2081	0.3130	0.0610
	243.6	0.3967	0.2076	0.6646	0.0709
	267.0	0.7140	0.2081	1.1398	0.0816
	290.0	1.0054	0.2102	1.5641	0.0911
	322.7	1.7107	0.2090	2.5530	0.1055
0.5063	163.0	0.1761	0.5012	0.3419	0.1210
	198.0	0.4470	0.5087	0.8002	0.1416
	228.6	0.7447	0.5004	1.2919	0.1487
	251.6	1.0564	0.5029	1.7767	0.1585
	316.2	2.6547	0.5123	4.0541	0.1972
	280.8	1.5352	0.5021	2.4496	0.1743
	350.6	4.4273	0.5270	6.5999	0.2261
	370.5	8.0667	0.5067	11.2414	0.2807

TABLE 7 (continued)

1.4464	230.5	2.0722	1.4416	3.5684	0.4147
	251.8	2.0714	1.4540	4.5159	0.4459
	282.5	3.8569	1.4130	6.0897	0.4648
	306.0	5.4036	1.4299	8.4371	0.5017
	322.5	6.9296	1.4167	10.4162	0.5549
	377.5	18.2547	1.4113	25.1282	0.6410
1.4531	116.8	0.2277	1.4854	0.5801	0.3217
	153.5	0.6708	1.4531	1.2893	0.3368
	190.5	1.2728	1.4716	2.300	0.3800
	186.0	1.1460	1.4395	2.0713	0.3658
	226.5	1.9955	1.4400	3.3845	0.4059
	277.0	2.8035	1.4474	6.0306	0.4730
	320.0	6.8557	1.4433	10.2680	0.5639

APPENDIX IV

P-x-y EXPERIMENTAL DATA

To obtain mole ratio from experimental observations, peak ratio of Appendix lll, Equations, (21), (22), and (23) were used for the binary system and Equation (26) and (27) were needed for the ternary system.

Calculation of mole fraction were then easily determined from Equations (24) and (25), and Equations (28), (29) and (30) for the binary and ternary systems respectively.

Tables 8(a, b, c) and Table 9 give the P-x-y data for each of the isotherms investigated.

TABLE 8a

BINARY SYSTEM Ar-CH_4 TEMPERATURE : 115.22°K

P(psia)	x_a	y_a
26.8	0.0440	0.2640
34.8	0.1051	0.4689
36.0	0.1169	0.4931
44.0	0.1695	0.5935
49.6	0.2206	0.6470
61.0	0.3328	0.7474
75.0	0.4354	0.8180
77.7	0.4806	0.8212
78.0	0.4748	0.8311
91.0	0.6153	0.8629
92.0	0.6015	0.8848
95.6	0.6581	0.8963
96.0	0.6560	0.8873
102.9	0.7245	0.9225
103.5	0.7084	0.9236
103.9	0.7292	0.9241
112.0	0.8019	0.9473
112.9	0.8068	0.9481
118.0	0.8610	0.9619
119.6	0.8756	0.9623
124.2	0.9155	0.9775
126.0	0.9313	0.9830
128.3	0.9531	0.9862

TABLE 8b

BINARY SYSTEM Ar-CH_4 TEMPERATURE :123.44°K

P(psia)	x_a	y_a
51.0	0.0621	0.3021
94.0	0.2896	0.6766
101.1	0.3494	0.7229
106.9	0.3717	0.7474
118.0	0.4472	0.7882
118.5	0.4333	0.7907
129.0	0.5004	0.8145
139.5	0.5756	0.8484
145.8	0.5987	0.8649
146.5	0.6087	0.8630
152.0	0.6446	0.8813
161.0	0.7015	0.9027
166.0	0.7242	0.9129
173.5	0.7684	0.9225
188.0	0.8580	0.9542
189.0	0.8670	0.9568
189.0	0.8616	0.9554
190.5	0.8739	0.9599
191.5	0.8796	0.9621

TABLE 8c

BINARY SYSTEM $Ar-CH_4$ TEMPERATURE :137.07

P(psia)	x_a	y_a
98.4	0.0403	0.1694
107.0	0.0756	0.2808
119.5	0.1136	0.3710
144.0	0.1942	0.4972
172.8	0.2948	0.6133
172.0	0.2918	0.6145
227.5	0.4704	0.7514
264.8	0.5967	0.8194
293.4	0.6850	0.8617
321.4	0.7680	0.8993
345.6	0.8359	0.9298
358.0	0.8696	0.9440
378.4	0.9270	0.9674

TABLE 9

TERNARY SYSTEM: A_7-N_2 - CH_4

TEMPERATURE 123.44°K

x_c/x_a for x_n=0		PRESSURE psia	x_a	x_n	x_c	y_a	y_n	y_c
0.1830	1	191.3	0.7025	0.0873	0.2102	0.7630	0.1749	0.0621
	2	200.0	0.6764	0.1209	0.2026	0.7121	0.2291	0.0587
	3	212.7	0.6361	0.1728	0.1911	0.6398	0.3093	0.0509
	4	231.9	0.5815	0.2482	0.1703	0.5456	0.4075	0.0469
	5	255.0	0.5062	0.3452	0.1486	0.4459	0.5116	0.0425
0.2095	1	202.2	0.6441	0.1381	0.2178	0.6791	0.2554	0.0655
	2	243.6	0.5497	0.2649	0.1854	0.5146	0.4276	0.0578
	3	267.0	0.4474	0.4013	0.1513	0.3839	0.5664	0.0497
	4	290.0	0.3801	0.4900	0.1299	0.3109	0.6441	0.0450
	5	322.7	0.2763	0.6299	0.0938	0.2149	0.7489	0.0362
0.5063	1	163.0	0.4861	0.1008	0.4131	0.6227	0.2568	0.1205

TABLE 9 (continued)

x_c/x_a for $x_n=0$		PRESSURE psia	x_a	x_n	x_c	y_a	y_n	y_c
	2	198.0	0.4150	0.2267	0.3583	0.4465	0.4520	0.1015
	3	228.5	0.3589	0.3366	0.3045	0.3416	0.5767	0.0817
	4	251.6	0.3113	0.4233	0.2655	0.2756	0.6541	0.0703
	5	280.8	0.2576	0.5231	0.2193	0.2166	0.7225	0.0610
	6	316.2	0.1818	0.6601	0.1581	0.1435	0.8106	0.0459
	7	350.6	0.1237	0.7654	0.1109	0.0934	0.8721	0.0344
	8	370.5	0.0751	0.8604	0.0645	0.0570	0.9166	0.0263
1.4464	1	230.5	0.1564	0.4371	0.4066	0.1505	0.7447	0.1047
	2	251.8	0.1363	0.5063	0.3575	0.1240	0.7830	0.0931
	3	282.5	0.1122	0.6019	0.2859	0.0963	0.8281	0.0756
	4	306.0	0.0894	0.6799	0.2307	0.0722	0.8664	0.0614
	5	322.5	0.0748	0.7341	0.1911	0.0595	0.8842	0.0563

TABLE 9 (continued)

x_c/x_a for x_n=0		PRESSURE psia	x_a	x_n	x_c	y_a	y_n	y_c
	6	377.5	0.0338	0.8810	0.0854	0.0261	0.9451	0.0288
1.4531	1	116.8	0.2531	0.0684	0.6785	0.4441	0.3195	0.2365
	2	153.5	0.2242	0.1881	0.5877	0.3084	0.5195	0.1720
	3	186.0	0.1968	0.2921	0.5110	0.2271	0.6345	0.1384
	4	190.5	0.1881	0.3125	0.4995	0.2103	0.6563	0.1334
	5	226.5	0.1592	0.4274	0.4134	0.1572	0.7359	0.1069
	6	277.0	0.1124	0.5942	0.2935	0.0970	0.8255	0.0775
	7	320.0	0.0751	0.7292	0.1956	0.0602	0.8819	0.0579

APPENDIX V

CONSISTENCY TEST

AND

PRELIMINARY TREATMENT OF EXPERIMENTAL DATA

Table 10 shows the results of Chang and Lu's general consistency test [23] when applied to the ternary system. This table indicates the non-consistent experimental points of the 123.44°K isotherm for the system $Ar-N_2-CH_4$.

TABLE 10

CONSISTENCY TEST ON THE TERNARY SYSTEM

TEMPERATURE 123.44 °K

ERROR IN PRESSURE: 0.5 psia

ERROR IN TEMPERATURE: 0.5 °K

NO. OF CONSISTENT POINTS	ERROR IN COMPOSITION E(x)	EXPERIMENTAL POINTS REJECTED (The number refer to those of Table 9 in appendix IV)				
		A	B	C	D	E
9	0.0005	4,5	1,4,5	1-8	1-6	5-7
10	0.0010	4,5	1,4,5	1,3-8	1-6	5-7
15	0.0015	-	1,4,5	5-8	1-6	5-7
19	0.0020	-	1,4,5	5-8	5,6	5-7
23	0.0025	-	1,5	5,7	6	6,7
27	0.0030	-	1	-	6	6,7

Table 11 shows the Redlich-Kister parameters obtain from activity coefficients calculated by the four proposed methods. Accompanying these constants are the standard deviation in the activity coefficients of methane and argon. The figures shown are those of minimum standard deviation in γ_i ; higher suffix-equations would have higher values of α_i .

Also listed are the percent average deviation in γ for CH_4 and Ar,

$$\%Da = \frac{\sum (\gamma_a^{calc} - \gamma_a^{obs})}{N}$$

TABLE 11

REDLICH-KISTER PROPERTIES RESULTING FROM ACTIVITY

COEFFICIENT DETERMINATION OF EXPERIMENTAL DATA

ISOTHERM TEMPERATURE (°K)		LOW PRESSURE Y_i FROM PRAUSNITZ' CORRELATION OF β_{ii}	LOW PRESSURE Y_i FROM BYRNE'S EXPERIMENTAL β_{ii}	HIGH PRESSURE Y_i FROM LYCKMAN'S $f^{\circ}_{i,L}$ CORRELATION	HIGH PRESSURE Y_i FROM CHUEH'S $f^{\circ}_{i,L}$ CORRELATION
90.67	B	0.1792	-	0.1502	0.1801
	α_a	0.0116	-	0.0209	0.0121
	α_c	0.0242	-	0.3515	0.0238
	%Da	0.63	-	1.51	0.65
	%Dc	1.46	-	22.00	1.39
115.22	B	0.1594	0.1610	0.1707	0.1589
	α_a	0.0271	0.0271	0.0848	0.0214
	α_c	0.0879	0.0878	0.0874	0.0872
	%Da	1.71	1.72	7.44	1.40
	%Dc	4.37	4.39	4.64	4.40
123.44	B	0.2187	0.1845	0.1474	0.1358
	α_a	0.1258	0.0671	0.0199	0.0288
	α_c	0.0993	0.0633	0.0479	0.0290
	%Da	8.73	4.55	1.00	1.49
	%Dc	7.02	4.56	3.41	2.04
137.07	B	0.1404	0.1404	0.1344	0.1329
	α_a	0.1642	0.1094	0.0288	0.0223
	α_c	0.2198	0.1235	0.0255	0.0163
	%Da	13.3	8.47	1.91	1.40
	%Dc	11.5	6.78	1.96	1.13

APPENDIX VI

OBSERVED AND CALCULATED LIQUID ACTIVITY COEFFICIENTS OF ARGON-METHANE SYSTEM

Table 12 (a,b,c) show the observed liquid activity coefficients, $\log \gamma_i^{obs}$, as calculated from Equations (12) and (18) for both components, argon and methane and the one-suffix Redlich-Kister Equation representation, $\log \gamma_i^{calc}$.

TABLE 12a

OBSERVED AND CALCULATED ACTIVITY COEFFICIENTS

TEMPERATURE: 115.22°K

REFERENCE FUGACITY
METHANE - 16.9 psia
ARGON - 112.2 psia

NO.	P	x_{Ar}	$\log\gamma_{Ar}^{obs}$	$\log\gamma_{CH_4}^{obs}$	$\log\gamma_{Ar}^{calc}$	$\log\gamma_{CH_4}^{calc}$
1	26.8	0.0440	0.1429	0.0109	0.1453	0.0003
2	34.8	0.1051	0.1226	0.0036	0.1273	0.0018
3	36.0	0.1169	0.1122	0.0028	0.1240	0.0022
4	44.0	0.1695	0.1138	0.0131	0.1097	0.0046
5	49.6	0.2206	0.0856	0.0261	0.0966	0.0077
6	61.0	0.3328	0.0527	0.0274	0.0708	0.0176
7	75.0	0.4354	0.0567	0.0340	0.0507	0.0301
8	77.7	0.4806	0.0293	0.0752	0.0429	0.0367
9	78.0	0.4758	0.0403	0.0980	0.0437	0.0360
10	91.0	0.6153	0.0042	0.1460	0.0235	0.0602
11	92.0	0.6015	0.0290	0.0592	0.0253	0.0575
12	95.6	0.6581	0.0101	0.0933	0.0186	0.0689
13	96.0	0.6560	0.0087	0.1280	0.0188	0.0684
14	102.9	0.7245	0.0085	0.0857	0.0121	0.0835
15	103.5	0.7084	0.0209	0.0568	0.0135	0.0798
16	103.9	0.7292	0.0100	0.0873	0.0117	0.0845
17	112.0	0.8019	0.0072	0.0895	0.0062	0.1022
18	112.9	0.8068	0.0079	0.0963	0.0059	0.1035
19	118.0	0.8610	0.0020	0.1194	0.0031	0.1179
20	119.6	0.8756	-0.0002	0.1672	0.0025	0.1219
21	124.2	0.9155	-0.0009	0.1231	0.0011	0.1333
22	126.0	0.9313	-0.0010	0.0958	0.0008	0.1379
23	128.3	0.9531	-0.0012	0.1766	0.0003	0.1444

TABLE 12b

OBSERVED AND CALCULATED ACTIVITY COEFFICIENTS

TEMPERATURE: 123.44°K

REFERENCE FUGACITY
METHANE - 33.1 psia
ARGON - 166.2 psia

NO.	P	x_{Ar}	$\log\gamma_{Ar}^{obs}$	$\log\gamma_{CH_4}^{obs}$	$\log\gamma_{Ar}^{calc}$	$\log\gamma_{CH_4}^{calc}$
1	51.0	0.0621	0.1525	0.0154	0.1195	0.0005
2	94.0	0.2896	0.0768	0.0318	0.0685	0.0114
3	101.1	0.3494	0.0519	0.0289	0.0575	0.0166
4	106.9	0.3717	0.0607	0.0232	0.0536	0.0188
5	118.5	0.4333	0.0573	0.0215	0.0436	0.0255
6	118.0	0.4472	0.0406	0.0360	0.0415	0.0272
7	129.0	0.5004	0.0391	0.0517	0.0339	0.0340
8	139.5	0.5756	0.0244	0.0602	0.0245	0.0450
9	145.8	0.5987	0.0316	0.0483	0.0219	0.0487
10	146.5	0.6087	0.0252	0.0667	0.0208	0.0503
11	152.0	0.6446	0.0225	0.0578	0.0172	0.0564
12	161.0	0.7015	0.0164	0.0647	0.0121	0.0668
13	166.0	0.7242	0.0181	0.0600	0.0103	0.0712
14	173.5	0.7684	0.0121	0.0977	0.0073	0.0802
15	188.0	0.8580	0.0059	0.1045	0.0027	0.1000
16	189.0	0.8616	0.0064	0.1055	0.0026	0.1008
17	189.0	0.8670	0.0043	0.1090	0.0024	0.1021
18	190.5	0.8735	0.0049	0.1020	0.0022	0.1037
19	191.5	08796	0.0048	0.0990	0.0020	0.1051

TABLE 12c

OBSERVED AND CALCULATED ACTIVITY COEFFICIENTS

TEMPERATURE: 137.07°K

REFERENCE FUGACITY
METHANE - 70.8 psia
ARGON - 274.3 psia

NO.	P	x_{Ar}	$\log\gamma_{Ar}^{obs}$	$\log\gamma_{CH_4}^{obs}$	$\log\gamma_{Ar}^{calc}$	$\log\gamma_{CH_4}^{calc}$
1	95.4	0.0403	0.1337	0.0010	0.1225	0.0002
2	107.0	0.0756	0.1244	0.0033	0.1136	0.0008
3	119.5	0.1136	0.1110	0.0038	0.1045	0.0017
4	144.0	0.1942	0.0757	0.0048	0.0863	0.0050
5	172.8	0.2948	0.0522	0.0086	0.0661	0.0116
6	172.0	0.2918	0.0558	0.0040	0.0667	0.0113
7	227.5	0.4704	0.0333	0.0233	0.0373	0.0294
8	264.8	0.5967	0.0172	0.0420	0.0216	0.0473
9	293.4	0.6850	0.0109	0.0589	0.0132	0.0624
10	321.4	0.7680	0.0067	0.0737	0.0072	0.0784
11	345.6	0.8359	0.0049	0.0816	0.0036	0.0929
12	358.0	0.8696	0.0038	0.0897	0.0023	0.1005
13	378.4	0.9270	0.0013	0.1161	010007	0.1143

APPENDIX V11

TERNARY EFFECT IN

ARGON-NITROGEN-METHANE SYSTEM

The ternary effect in $Ar-N_2-CH_4$ system was analysed. The basis for analysis was the consistent points obtained as the error in composition, E(x), varied from 0.0005 to 0.0030 . For the sake of comparison, the smoothed and the experimentally determined B_{Ar-CH_4} were selected from B_{ij} vs $1/T$ curve of Figure (8). Furthermore, the ternary constants were determined from Lyckman's correlation of $f_{i,L}^{\circ}$ and Equation (18).

The results of such study were compiled in Table 13 .

TABLE 13

TERNARY EFFECT IN Ar-N_2-CH_4 SYSTEM

Parameter : Error in composition, E(x)

Constants : Error in pressure , E(p)=0.5 psia

Error in temperature, E(T)=0.5°K

$\overline{C}_{123}$ calculated from Equations (25) and (26) from a one-term Redlich-Kister Equation.

B_{Ar-CH_4} =		0.1521		0.1474 (smooth)	
E(x)	No.Pts.	$\overline{C}_{123}$	α	$\overline{C}_{123}$	α
0.0005	9	1.62	1.63	1.65	1.62
0.0010	10	1.60	1.54	1.63	1.52
0.0015	15	1.80	1.49	1.83	1.48

$\overline{C}_{123}$ calculated from Equations (25) and (26) from a two-term Redlich-Kister Equation.

B_{Ar-CH_4} =		0.1475		0.1475 (smooth)	
C_{Ar-CH_4} =		-0.0310		-0.0017	
E(x)	No.Pts.	$\overline{C}_{123}$	α	$\overline{C}_{123}$	α
0.0005	9	0.560	1.98	0.57	1.94
0.0010	10	0.57	1.87	0.59	1.83
0.0015	15	0.78	1.77	0.80	1.74